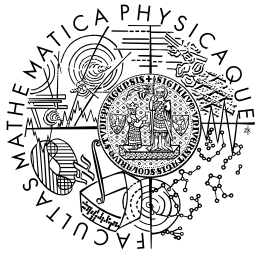

FACULTY
OF MATHEMATICS
AND PHYSICS
Charles University

BACHELOR THESIS

Daniel Herman

Electron-phonon Coupling in Finite Multi-chromophoric Systems

Institute of Physics of Charles University

Supervisor of the bachelor thesis: doc. RNDr. Tomáš Mančal, Ph.D.

Study programme: General Physics

Prague 2020

I declare that I carried out this bachelor thesis independently, and only with the cited sources, literature and other professional sources. It has not been used to obtain another or the same degree.

I understand that my work relates to the rights and obligations under the Act No. 121/2000 Sb., the Copyright Act, as amended, in particular the fact that the Charles University has the right to conclude a license agreement on the use of this work as a school work pursuant to Section 60 subsection 1 of the Copyright Act.

In ..... date ....

Author's signature

I would like to thank my supervisor Tomáš Mančal for his guidance to the world of science and also my friends and colleagues for fruitful discussions.

Title: Electron-phonon Coupling in Finite Multi-chromophoric Systems

Author: Daniel Herman

Department: Institute of Physics of Charles University

Supervisor: doc. RNDr. Tomáš Mančal, Ph.D., Institute of Physics of Charles University

Abstract: Quantum systems in nature interact with other quantum systems, and these are examples of open quantum systems. In this work, we provide an introduction to the theory of open quantum system with a particular focus on the dynamics of molecular systems embedded in the protein environment, such as those found in photosynthetic antennas. We devote some time to the techniques of constructing equations of motion for the dynamics of a selected quantum system under the interaction with the bath, where we restrict ourselves to a finite number of degrees of freedom. We compare the exact calculation of the whole finite system with the results of approximate equations derived from an ansatz for the time evolution for the degrees of freedom of the bath part. We also reformulate the exact equations into a time non-local master equation using projection operator techniques, and we study the quality of results obtained with the modified quantum master equation. The time evolution of studied systems is also compared to the time evolution obtained by Schrödiger and Liouville-von Neumann equations.

Keywords: open quantum systems, molecular aggregates, quantum master equation

Contents

1D - one-dimensional
2D - two-dimensional
DOF - degrees of freedom
FC - Franck-Condon
FMO - Fenna-Matthews-Olson photosynthetic pigment-protein complex
FT - fourier transform
HEOM - hierarchical equations of motion
IDE - integrodifferential equation
LHO - linear harmonic oscillator
ODE - ordinary differential equation
OQS - open quantum system
QME - quantum master equation
RDM - reduced density matrix
SBC - system-bath coupling
TL - time-local
TNL - time-nonlocal

1. Introduction

Quantum theory changed our understanding of how nature works inside out. In classical physics, trajectories in three-dimensional space, or in so-called phase-space, are defined by characteristic coordinates and momenta, which together determine the degrees of freedom of macroscopic bodies. Quantum theory is suited for the description of microscopic bodies, where classical mechanics is insufficient. The fundamental change between the classical and qauntum theories, however, lies in the definition of what is the physical state of the system. In the quantum mechanical description, coordinates and momenta can not be determined precisely at the same time, as they have to obey the Heisenberg uncertainty principle. All characteristics of the system are set by Hilbert space wave-function or state-vector. As every system is defined on its own Hilbert space, the composed system is defined on the product of all Hilbert spaces of its contributions. Correspondingly, the total state-vector becomes astonishingly complex as we strive for a description of gradually bigger systems. Another aspect of the description of such systems is the entanglement with the surrounding systems. With an expanding system, it is harder to separate it from its surroundings. Small molecular systems of interest, i.e. in the theory of photosynthetic antennas, show coherence dephasing times on the order of hundreds of femtosenconds. The state-vector of the system quickly becomes entangled with the rest of the universe, which prevents us from defining it as a quantity describing the system alone [CCC$^+$20, Man20].

The theory of open quantum systems is dealing with the influence of the enviroment or bath. We choose a few degrees of freedom (DOF), which are described in fine detail and call them the system. The rest of the DOF represent the universe and thus becomes implicit in the description. Open quantum systems in nature have one critical property in common, namely, the irreversibility of time evolution, which is due to the interaction of infinite bath surrounding the system. A natural external perturbation of our interest is caused by the interaction of the system with the electromagnetic field. As the transition frequencies of the system match the frequencies of the electromagnetic field, the resonance condition is fulfilled, the energy is transferred to the system, which becomes exited. After the system is excited, the decoherence, energy relaxation and thermalization take place. Spectroscopy and in particular time-resolved spectroscopy is an excellent experimental tool for monitoring such features and properties of the system. Molecular aggregates play an essential role in natural photosynthesis, where photosynthetic antennae composed of pigment molecules absorb light [Bla95]. These antennae enable cells and bacteria to catch light more efficiently as the antenna has a broader cross-section than individual pigment molecules. Energy is transferred into the reaction centre after photons are harvested. Ultrafast time evolution of electronic states of molecular aggregates is the subject of study of non-linear optical spectroscopy, which noted many new advantages. In particular the two-dimensional coherent spectroscopy [Jon03, COM04, BMSF04] in infra-red regions, and in visible regions of spectra, permit us to obtain information about third-order non-linear response. The time resolution of pump-probe experiments is limited by the frequency resolution and *vice versa*. This is not the case of two-dimensional spectroscopy, which allows us not only to determine

the population of Frenkel excitons but also their composition in terms of quantum superposition. These superpositions of electronic states are represented by off-diagonal elements of the reduced density matrix, which are also called coherences. The reduced density matrix is obtained from the density matrix of the whole system with tracing out the degrees of freedom of the bath. Experiments which were carried out with the Fenna-Matthews-Olson pigment-protein complex confirmed the presence of such coherences in natural systems [ECR+07].

Modelling molecular aggregate spectroscopic response is a challenging task as we need to simulate the time evolution of the whole system. Because the Hilbert space of the system and the bath are not linearly separable, we can not apply the Schrödinger equation in the usual way. The Quantum Master Equation can be derived, e.g. by Nakajima-Zwanzig projection formalism [Fai02], and it answers the exact time evolution of the system. However, it is an integrodifferential equation that cannot be easily solved numerically. Approximations, namely Born approximation and Markov approximation with strong coupling, are used in order to overcome this difficulty, and we obtain Redfield rate equations [Red65]. Master equation theory can be further reduced to simpler rate theories by another approximation called secular approximation, which decouples the coherence of the reduced density matrix. These approximations make it possible to simulate an open quantum system interacting with a bath. However, the weak part of these theories are many fair assumptions about the bath, necessary due to its infinite nature. In order to provide a test-bed for improvements of master equations, we simulate finite baths. We strive for obtaining new equations of motion in the case that the bath is finite and comparable to the size of the system degrees of freedom.

In this work, we will perform exact calculations of the dynamics of finite systems, which can be reasonably split into an effective system, and a finite bath. We derive equations of motion with one ansatz for the bath time evolution. Numerical results of these new set of equations will be compared to the exact dynamics obtained by Liouville-von Neumann equation and quantum master equations. As the system and the number of bath degrees of freedom are expanding with the motivation to catch the essential aspects of the mentioned experiments, the total basis of the system grows exponentially. After the evolution is calculated, we have to extract meaningful information from this vast number of degrees of freedom, which is usually done by tracing out the degrees of the bath. As we will show later in this work, this operation can be computationally more intensive than the time evolution itself. It is crucial to deal with these new problems, in such a way, that the simulation overall remains feasible and practical.

2. Open Quantum Systems

2.1 Density Operator Formalism

To learn something new about the underlying principles of quantum systems which are the subject of this study, it is inevitable to use density operator formalism. The formalism of quantum mechanics, which uses purely wave formalism, can make predictions only on an ensemble - that, is a collection of identically prepared physical systems. In such an ensemble, the same vector state characterises all members $|\psi\rangle$. We aim to study open quantum systems, which are surrounded by a greater system (reservoir or bath). The total wave function of such a system is $\psi(s_i, b_j) \in \mathcal{H}$, where $\mathcal{H}$ is Hilbert space with a given basis, s_i are DOF of the inner open system and b_i are DOF of the bath. In case the system is non-interacting with the reservoir, it is possible to separate the basis into $\psi_{\mathrm{S}}(s_i)\,\psi_{\mathrm{B}}(b_j)$ with $\psi_{\mathrm{S}}(s_i) \in \hat{\mathcal{H}}_{\mathrm{S}}$ and $\psi_{\mathrm{B}}(b_j) \in \hat{\mathcal{H}}_{\mathrm{B}}$. However, when the system and bath are interacting with one another, it is impossible to separate the basis and hence the wave function. We will illustrate this on a simple example with the Stern-Gerlach experiment. At the beginning of an experiment, a person prepared two electrons with state $|\psi_1\rangle$ and after the experiment took place, the electrons are now in state $|\psi_2\rangle$

$$|\psi_1\rangle = |\uparrow\rangle\,|\uparrow\rangle\,, \quad |\psi_2\rangle = \frac{1}{2}\,|\uparrow\rangle\,|\uparrow\rangle + \frac{1}{2}\,|\downarrow\rangle\,|\downarrow\rangle\,. \tag{2.1}$$

The initial state of two electrons can be separated into $|\psi_i\rangle = |\uparrow\rangle$; however, it is impossible to separate the second state. Omitting superposition of states essentially ties our hands, and the suitable step is to change our perception of a given problem. The second state is called a mixed state, which is described by the density operator formalism [Sak10].

Now we present density operator formalism, pioneered by J. Neumann in 1927, that quantitatively describes physical situations with mixed states of the system. The density operator of the system is characterised in general by elements $|\alpha_i\rangle$ of some basis with coefficients w_i which obey the following condition

$$1 = \sum_i w_i. \tag{2.2}$$

Suppose that we measure some observable B, then we would like to know what is the average value of B, when many measurements are carried out. That is given by

$$\begin{aligned} \langle \hat{B} \rangle &\equiv \sum_i w_i \,\langle \alpha_i | \hat{B} | \alpha_i \rangle \\ &= \sum_i \sum_j w_i \,|\langle \beta_j | \alpha_i \rangle|^2 \,\beta_j, \end{aligned} \tag{2.3}$$

where $|\beta_j\rangle$ are eigenstates of operator $\hat{B}$ and $\langle \alpha_i | \hat{B} | \alpha_i \rangle$ is quantum mechanical expectation value with respect to the state $|\alpha_i\rangle$. Motivation is to define density operator $\hat{\rho}$ as

$$\hat{\rho} \equiv \sum_i w_i \,|\alpha_i\rangle\langle\alpha_i|\,. \tag{2.4}$$

The elements of the corresponding density matrix in basis $|b_i\rangle$ have the following form

$$\langle b_i|\hat{\rho}|b_j\rangle = \sum_k w_i \langle b_i|\alpha_k\rangle \langle \alpha_k|b_j\rangle . \tag{2.5}$$

For pure state there exist such an n that

$$\hat{\rho} = |\alpha_n\rangle\langle\alpha_n| . \tag{2.6}$$

The density operator contains all physically significant information that we can obtain, we can rewrite the average of the operator as follows

$$\begin{aligned}\left[\hat{B}\right] &\equiv \sum_i \sum_j \langle b_j|\hat{\rho}|b_i\rangle \ \langle b_i|\hat{A}|b_j\rangle \\ &= \mathrm{Tr}\Big\{\hat{\rho}\hat{A}\Big\}.\end{aligned} \tag{2.7}$$

Another important fact is that we can evaluate the trace in any given basis, which can be convenient.

2.1.1 Interaction Picture

The two main ways how to look at the so-called quantum system and work with all so-calledinformation about system dynamics are Schrödinger picture or by interaction picture. In the so-called Schrödinger picture, all system information is held in time-dependent coefficients of wave-vector $|\psi(t)\rangle$ with respect to some basis $\{|n\rangle\}_{n=0}^{\infty}$. We consider a Hamiltonian H such that it can be split into two parts,

$$H = \hat{H}_0 + V(t), \tag{2.8}$$

where $\hat{H}_0$ does not contain time explicitly. If we assume a problem where $V(t) = 0$, the dynamics can be formally solved by finding energy eigenkets $|n\rangle$ and correspondent eigenvalues E_n, which are defined by

$$\hat{H}_0 |n\rangle = E_n |n\rangle . \tag{2.9}$$

We may possibly be interested in a simulation where at the beginning only one of the states, to give an example, $|i\rangle$, is populated. However, if we assume that $V(t) \neq 0$, generally speaking, other states will become populated too. The evolution operator is no longer as simple as $e^{-iHt/\hbar}$ when H is time-dependent. Suppose that at $t = 0$ the wave-vector is given by

$$|\psi(t=0)\rangle = \sum_n c_n(0) |n\rangle . \tag{2.10}$$

To solve the dynamics of such a system means that we need to find such $c_n(t)$ for $t \geq 0$ so we can write wave-vector as

$$|\psi(t)\rangle = \sum_n c_n(t) e^{-iE_n t\ \hbar} |n\rangle . \tag{2.11}$$

For operators (which represent observables) we define

$$A_I \equiv e^{i\hat{H}_0 t/\hbar} A_S e^{-i\hat{H}_0 t/\hbar}. \tag{2.12}$$

For operators that are time-independent in Schrödinger picture we sometimes omit the subscript I and use the time-dependence of the operators alone to indicate that they are in the interaction picture.

2.2 Superoperators

2.2.1 Liouville-von Neumann Equation

The subject of the study is the time evolution of the density matrix operator, we shall start with the pure state and later we will show that the derived equation holds for mixed states as well. The time derivative of the density matrix operator consists of a sum of contributions from the bra state and from ket state

$$\frac{\partial \rho}{\partial t} = \left(\frac{\partial}{\partial t} |\psi(t)\rangle \right) \langle \psi(t)| + |\psi(t)\rangle \left(\frac{\partial}{\partial t} \langle \psi(t)| \right). \tag{2.13}$$

Using the Schrödinger equation and its Hermitian conjugate we can state

$$\frac{\partial}{\partial t} |\psi\rangle = -\frac{i}{h} \hat{H} |\psi\rangle , \quad \frac{\partial}{\partial t} \langle \psi| , = \frac{i}{h} \hat{H} \langle \psi| \tag{2.14}$$

and we can rewrite 2.13 using operators of system Hamiltonian $\hat{H}$ as

$$\begin{aligned} \frac{\partial \rho}{\partial t} &= -\frac{i}{\hbar} \hat{H} |\psi\rangle\langle\psi| + \frac{i}{\hbar} |\psi\rangle\langle\psi| \hat{H} \\ &= -\frac{i}{\hbar} (\hat{H}\rho - \rho\hat{H}). \end{aligned} \tag{2.15}$$

The equation of motion for density matrix we derived above is called the Liouville-von Neumann equation of motion

$$\frac{\partial \rho}{\partial t} = -\frac{i}{\hbar} [\hat{H}, \rho]. \tag{2.16}$$

We are motivated to define a new category of operators for the simplicity of notation such that

$$\mathcal{L}(\,\cdot\,) \equiv \frac{1}{\hbar} \left[\hat{H}, \,\cdot\, \right], \quad \frac{\partial}{\partial t} \rho(t) = -i\mathcal{L}\rho(t), \tag{2.17}$$

where $\mathcal{L}$ is so-called Liouville superoperator or Liouvillian and this operator is defined on co-called Liouville space [Bre02]. Given some Hilbert space, $\mathcal{H}$ the Liouville space is the space of Hilbert-Schmidt operators, which is the space of operators A in $\mathcal{H}$ for which $\mathrm{Tr}\left\{A^\dagger A\right\}$ is finite. With the scalar product

$$(A, B) \equiv \mathrm{Tr}\left\{A^\dagger B\right\}, \tag{2.18}$$

the space of Hilbert-Schmidt operators becomes a Hilbert space itself. It is plausible to introduce orthonormal basis $\{B_i\}$ in this space which satisfies orthonormality and completeness condition

$$\begin{aligned} (B_i, B_j) &= \delta_{ij} \\ A &= \sum_i B_i \, (B_i, A) \, . \end{aligned} \tag{2.19}$$

2.2.2 Superoperator Representation

Our superoperators applied on density matrix are represented in a finite basis by tensors of rank four. It is desirable to represent these superoperators with matrices and density operators with vectors. After the theory is derived, simulations will take place and it is inevitable to restrict ourselves to a finite basis. There seem to be many practical advantages of using matrices and vectors instead of multidimensional arrays. A reader can choose suitable mapping for this description of the representation issue

$$(\mathcal{L}_{ij,kl}) = (\mathcal{L}_{a,b}), \quad a = M(i,j), b = M(k,l). \tag{2.20}$$

The simplest possible mapping would be Vectorization/Choi-Jamiolkowski isomorphism [Jam72]. What is neatly captured in following relation

$$|i\rangle\langle j| = |i\rangle \otimes |j\rangle . \tag{2.21}$$

In this way, when we have an arbitrary density matrix

$$\rho = \sum_{i,j} \rho_{i,j} |i\rangle\langle j| , \tag{2.22}$$

represented in a vector form as follows

$$\mathrm{vec}(\rho) = \sum_{i,j} \rho_{i,j} |i\rangle \otimes |j\rangle . \tag{2.23}$$

If we represent these objects in a given basis, we are "stacking columns of the matrix".

$$\mathrm{vec} \begin{pmatrix} a & b \\ c & d \end{pmatrix} = \begin{pmatrix} a \\ c \\ b \\ d \end{pmatrix} . \tag{2.24}$$

This vectorization trick is handy, in particular for one main reason. The Hilbert-Schmidt inner product can be represented by what one would intuitively guess

$$\mathrm{tr}\left(A^\dagger B\right) = \mathrm{vec}(A)^\dagger \,\mathrm{vec}(B), \tag{2.25}$$

which becomes merely the inner product between the two vectors.

2.2.3 Projection Superoperators

The laws describing the dynamics of the open quantum system interacting with the bath can be derived from the unitary dynamics of the total system. Reducing degrees of freedom usually results in non-Markovian behaviour. Using projection operator techniques, one can still derive exact equations of motion. Nakajima introduced these techniques in 1958 and Zwanzig in 1960 ([Nak58], [Zwa60]) and it was independently introduced by the Brussels school (Prigogine, 1962 [Pri17]).

The basic idea underlying the application of the projection operator is to trace out degrees of freedom originating from the bath with formal projection $\rho \to \mathcal{P}\rho$.

The superoperator $\mathcal{P}$ has the property of projection operator on normal Hilbert space, which is $\mathcal{P}^2 = \mathcal{P}$. The density matrix $\mathcal{P}\rho$ is called a *relevant part* of the density matrix. Similarly, we define $\mathcal{Q} = 1 - \mathcal{P}$ and we call $\mathcal{Q}\rho$ as *irrelevant part* of the density matrix. The next step would be to derive closed differential equations for the relevant part of the density matrix $\mathcal{P}\rho$.

In regular Hilbert space, we have projector onto n-th state $\hat{P}_{\mathrm{S}}$ as follows

$$\left(\hat{P}_n\right)_{ij} \equiv \delta_{in}\delta_{jn}. \tag{2.26}$$

Correspondingly projection superoperator, acting on some operator $\mathcal{A}$, is from Liouville space and its components are defined as

$$\left(\mathcal{P}^{ij,kl}\mathcal{A}\right)_{i'j',k'l'} \equiv \mathcal{A}_{ij,kl}\delta_{ii'}\delta_{jj'}\delta_{kk'}\delta_{ll'}. \tag{2.27}$$

In our work, we will be working also with superoperators of the following type

$$\mathcal{C}\rho = \hat{A}\rho\hat{B}, \tag{2.28}$$

where we can spot that some superoperator $\mathcal{C}$ has components $\mathcal{A}$ and $\mathcal{B}$. Now we want to project only the relevant part of this operator. We can do it in the following way

$$\mathcal{P}^{ij,kl}\mathcal{C} = \hat{P}_i\hat{A}\hat{P}_k\rho\hat{P}_l\hat{B}\hat{P}_j. \tag{2.29}$$

The reader should keep in mind that with the basis of size N in Hilbert space, the size of the general superoperator is N^4. However, the properties of superoperators usually allow us to write them down as nested sums working on Hilbert space. That being said, 2.29 can be easily expressed in terms of sums iterating over elements of ρ.

2.3 The Definition of Open System and Bath

Quantum chemistry methods currently represent the only valid alternative to spectroscopic techniques to study structural and electronic properties of molecular systems. There appear to be plenty of MO-based models, e.g. Hartree-Fock, which aims for a relevant description of photosynthetic models. Many alternative models have been proposed to achieve a better description of larger systems. Considerable effort has been focused on obtaining methods accounting for electronic transfer that in HF and similar conventional quantum chemistry methods were neglected [Cro18].

Molecular systems of our interest can be described with relatively small amounts of DOF, but these DOF are described in exquisite detail. We shall call these DOF *system* or *open system*, and we want to use a full quantum description of these DOF. Other DOF which take place in the model also plays an important role, as an example in decoherence and relaxation towards equilibrium. It is necessary to use less detailed descriptions for these DOF, and we call them *bath*. The open system and the bath together create *whole system*. Next, we denote Hilbert space of the system and Hilbert space of the bath as $\mathcal{H}_{\mathrm{S}}$ and $\mathcal{H}_{\mathrm{B}}$ respectively.

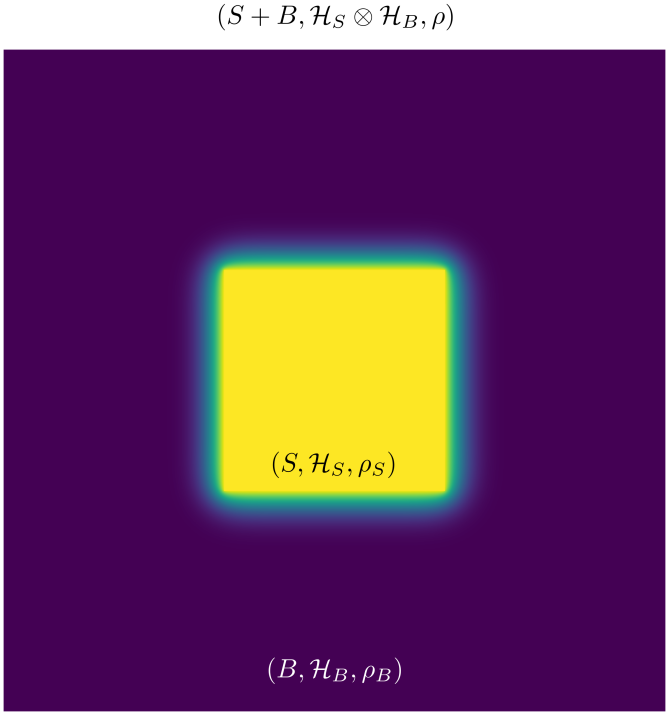

Figure 2.1: Open quantum system is entangled with the surrounding bath after some time.

The subject of this study is focused on exciton systems. Among the photosynthetic complexes, there appear to be many systems which consist of Chlorophyll molecules embedded in a protein with a different structure (LHI, LH2, FMO, and other). We can model these aggregates with N molecules which have two states: the ground state $|g\rangle$ and the excited state $|e\rangle$. The tensor product of these states then creates DOF of the whole system. If we take into account vibrational degrees of freedom of these molecules, we will state that in a particular model. The global aggregate electronic states have a form

$$\begin{aligned} |g\rangle &= \prod_{i=1}^{N} |g\rangle \,, \\ |e_n\rangle &= |e_n\rangle \prod_{\substack{i=1 \\ i\neq n}}^{N} |g_i\rangle \,, \end{aligned} \tag{2.30}$$

molecule and by $|e_i\rangle$ we denote the excited state of n-th molecule. We are interested only in modelling non-linear spectroscopy experiments up to third order in electronic field density. Therefore, we can neglect any higher excited states than one excited.

Specific desire after a simple description of vibrational basis plays a role in effective theory derivation and consequent implementation. Every oscillator in bath induces its locally orthogonal basis. It is unavoidable to restrict ourselves to a finite local basis; when it comes to performing simulations, for every n-th

molecule in the whole system we state N_{ξ_n} as the maximum number of states for both oscillator in the ground state and the excited state. The n-th vibrational state has the following form

$$|\xi_n\rangle = |\xi^{\mu_1}\rangle|\xi^{\mu_2}\rangle \dots |\xi^{\mu_p}\rangle, \tag{2.31}$$

here we assumed that p is the number of all molecules in the whole system. Together with the electronic state, we obtain

$$|n\rangle = |a\rangle|\xi_n\rangle = |\xi^{\mu_1}_{a_1}\rangle|\xi^{\mu_2}_{a_2}\rangle \dots |\xi^{\mu_p}_{a_p}\rangle, \tag{2.32}$$

where $|a\rangle$ can be the ground state $|g\rangle$ or the excited state $|e_k\rangle$.

2.4 Local and Excitonic Basis

As long as we are working within boundaries of Hilbert space, we are free to choose our own basis of states for calculations. Nevertheless, local and exciton basis are two bases of particular importance. In *exciton basis* is the system Hamiltonian $\hat{H}_{\mathrm{S}}$ diagonal and local basis has the form of 2.30.

With a local basis, every excited basis state is located on a particular molecule. Therefore, properties such as transition dipole, a coupling of molecules or the correlation of the energy gap fluctuations directly relate to the geometrical arrangement of the aggregate. The exciton basis is the natural choice in the case of a weakly coupled system to the bath, because the population of eigenstates of the system Hamiltonian, will change only slowly with time. We call these eigenstates excitons. Another aspect which we should take into account is thermalization, that drives the system towards canonical distribution

$$\rho_{\mathrm{eq}} = \frac{e^{-H/k_B T}}{\mathrm{Tr}\, e^{-H/k_{\mathrm{B}} T}}. \tag{2.33}$$

2.5 Franck - Condon Factors

In this section, we will establish a notation for the Franck-Condon factors and discuss what role they play in our model. We start with the Hamiltonian of LHO

$$\hat{H} = \frac{\hbar\omega}{2}\left(\hat{p}^2 + \hat{q}^2\right), \tag{2.34}$$

where $\hat{p}$ is the momentum operator, $\hat{q}$ is the position operator, and ω is the frequency of LHO. We would like to define a shift operator which acts on state vector as follows

$$D(\alpha)\psi(Q) = \psi(Q - \alpha), \tag{2.35}$$

where $\alpha \in \mathbb{R}$ is the shift value. Therefore, we define the shift operator as

$$\hat{D}(\alpha) = e^{-\alpha \frac{\partial}{\partial \hat{q}}}. \tag{2.36}$$

Unquestionably, we want to write the final result in eigenstates of LHO so we will use annihilation and creation operators with knowledge of the following identities

$$\begin{aligned} \hat{a} &= \tfrac{1}{\sqrt{2}}\left(\hat{q} + i\hat{p}\right) \quad \hat{q} = \tfrac{1}{\sqrt{2}}\left(\hat{a} + \hat{a}^\dagger\right) \\ \hat{a}^\dagger &= \tfrac{1}{\sqrt{2}}\left(\hat{q} - i\hat{p}\right) \quad \hat{p} = \tfrac{1}{i\sqrt{2}}\left(\hat{a} - \hat{a}^\dagger\right). \end{aligned} \tag{2.37}$$

Using these identities, we can now transform the shift operator in 2.36 into

$$\begin{aligned} \hat{D}(\alpha) &= e^{-i\alpha\hat{p}} \\ &= e^{-\frac{\alpha}{\sqrt{2}}\left(\hat{a}-\hat{a}^\dagger\right)}. \end{aligned} \tag{2.38}$$

Matrix elements of such operator $\hat{D}_\alpha$ in terms of LHO eigenstates are the so-called Franck-Condon factors $\langle i|\hat{D}_\alpha|j\rangle$. Eequation 2.38 is usefull in practical numerical evaluation. In appendix A.4, we will show that recurrent formulas may be practical when it comes to a higher number of eigenstates, however, for $N \leq 20$ the formula 2.38 is sufficient.

Later we will use Franck-Condon factors for general integrals of the type $\langle n|m\rangle$, where $|n\rangle$, $|m\rangle$ are states of the whole system as defined in 2.32. Assuming that we have p molecules in the whole system and each molecule has defined shift α_i between the ground state and the excited state, the Franck-Condon factors are defined as follows

$$\langle n|m\rangle = \prod_{i=1}^{p} \langle \mu_i|\hat{D}(e_{ni}\alpha_i - e_{mi}\alpha_i)|\nu_i\rangle\,, \tag{2.39}$$

where $e_{nk} = 1$ if k-th molecule of the aggregate is excited and $e_{nk} = 0$ otherwise. States $|\mu_k\rangle$, $|\nu_k\rangle$ are locally orthonormal states for k-th molecule in the aggregate for the ground or the excited state. The interested reader can find in the appendix A.4 how to evaluate multidimensional Franck-Condon factors for the whole system efficiently.

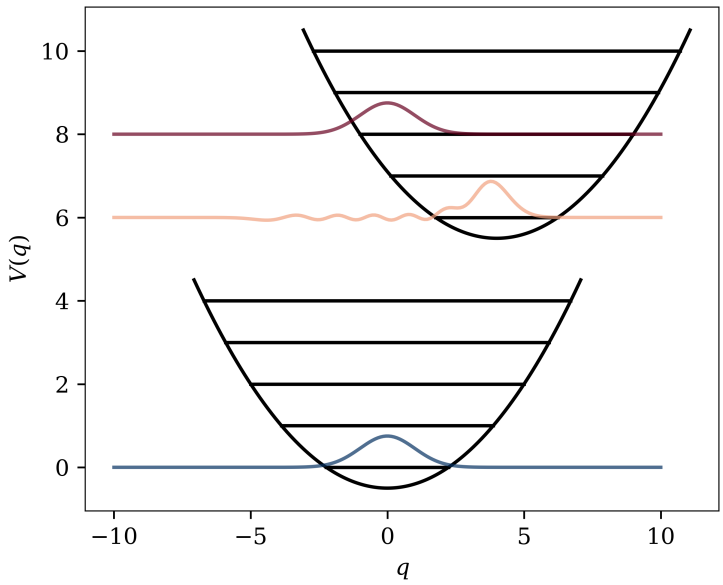

Figure 2.2: Gaussian wave-packet in the ground state and an excited state of LHO potential transformed using Franck-Condon factors.

2.6 Nakajima Zwanzig Identity

The purpose of this section is to derive suitable equations of motion for the reduced density operator $\hat{\rho}(t)$. The density operator of the whole system is denoted by $\hat{W}(t)$ as we mentioned in 2.2.3. We first try to find the equation of motion of the density matrix $\mathcal{P}\hat{W}(t)$. As shown below, formal equations can be derived in closedform. Solving these differential equations is equally tricky as solving the full dynamics for $\hat{W}(t)$, but it can be used as a starting point for a consequential approximate treatment [Val13]. The starting point will be Liouville von Neumann equation 2.17 with Liouville superoperator that corresponds to the Hamiltonian of the whole system

$$\frac{d}{dt}\hat{W}(t) = -\mathrm{i}\mathcal{L}\hat{W}(t). \tag{2.40}$$

At this point, we could rewrite equation 2.40 into interaction picture concerning $\mathcal{L}_{\mathrm{S}}$ and $\mathcal{L}_{\mathrm{B}}$, the meaning behind such a step would be to continue in perturbation expansion to $\mathcal{L}_{\mathrm{SB}}$ after derivation of Nakajima-Zwanzig equations are complete. Using the identity $1 = \mathcal{P} + \mathcal{Q}$ we can rewrite 2.40 as follows

$$\frac{d}{dt}(\mathcal{P}+\mathcal{Q})\hat{W}(t) = -i(\mathcal{P}+\mathcal{Q})\mathcal{L}(\mathcal{P}+\mathcal{Q})\hat{W}(t). \tag{2.41}$$

Under the properties of projection superoperators $\mathcal{P}$ and $\mathcal{Q}$ we can now separate

$$\begin{aligned}
\frac{d}{dt}\mathcal{P}\hat{W}(t) &= -i\mathcal{P}\mathcal{L}\mathcal{P}\hat{W}(t) - i\mathcal{P}\mathcal{L}\mathcal{Q}\hat{W}(t), \\
\frac{d}{dt}\mathcal{Q}\hat{W}(t) &= -i\mathcal{Q}\mathcal{L}\mathcal{P}\hat{W}(t) - i\mathcal{Q}\mathcal{L}\mathcal{Q}\hat{W}(t).
\end{aligned} \tag{2.42}$$

Pair of such ODE can be formally solved in a trivial manner, where from the second equation in 2.42 we obtain

$$\mathcal{Q}\hat{W}(t) = -ie^{-i\mathcal{Q}\mathcal{L}(t-t_0)}\mathcal{Q}\hat{W}\left(t_0\right) - i\int_{t_0}^{t} \mathrm{d}\tau e^{-iQ\mathcal{L}(t-\tau)}\mathcal{Q}\mathcal{L}\mathcal{P}\hat{W}(\tau), \tag{2.43}$$

and we plug it into the first equation of 2.42 obtaining the integrodifferential equation, also called Nakajima-Zwanzig identity in Schrödinger picture

$$\begin{aligned}
\frac{d}{dt}\mathcal{P}\hat{W}(t) = &- i\mathcal{P}\mathcal{L}\mathcal{P}\hat{W}(t) - \mathcal{P}\mathcal{L}e^{-i\mathcal{Q}\mathcal{L}(t-t_0)}\mathcal{Q}\hat{W}\left(t_0\right) \\
&- \mathcal{P}\mathcal{L}\int_0^{t-t_0} \mathrm{d}s e^{-i\mathcal{Q}\mathcal{L}s}\mathcal{Q}\mathcal{L}\mathcal{P}\hat{W}(t-s).
\end{aligned} \tag{2.44}$$

For the interaction picture, it would be desirable to transform 2.40 into the interaction picture with respect to $\mathcal{L}_{\mathrm{S}}$ and $\mathcal{L}_{\mathrm{B}}$. Here we assumed that the Liouvillian of the whole system is composed of three parts

$$\mathcal{L} = \mathcal{L}_{\mathrm{S}} + \mathcal{L}_{\mathrm{R}} + \mathcal{L}_{\mathrm{SB}}. \tag{2.45}$$

Using the interaction picture as mentioned in 2.1.1 and rewriting 2.40 we obtain

$$\frac{d}{dt}\hat{W}(t) = -\mathrm{i}\mathcal{L}\hat{W}(t). \tag{2.46}$$

As the reader is probably expecting, we could derive in a similar manner the full Nakajima-Zwanzig identity for the interaction picture, what would yield onto

$$\begin{aligned}\frac{d}{dt}\mathcal{P}\hat{W}^{(I)}(t) =& -i\mathcal{P}\mathcal{L}_{SB}(t)\mathcal{P}\hat{W}^{(I)}(t) \\ &- i\mathcal{P}\mathcal{L}_{\mathrm{SB}}(t)\exp_{+}\left(-i\int_{t_0}^{t}\mathrm{d}\tau\,\mathcal{Q}\mathcal{L}_{\mathrm{SB}}(\tau)\mathcal{Q}\right)\mathcal{Q}\hat{W}^{(I)}\left(t_0\right) \\ &- \int_{t_0}^{t}\mathrm{d}\tau\mathcal{P}\mathcal{L}_{\mathrm{SB}}(t)\exp_{+}\left(-i\int_{t_0}^{t-\tau}\mathrm{d}\tau'\mathcal{Q}\mathcal{L}_{\mathrm{SB}}\left(\tau'\right)\mathcal{Q}\right)\times \\ &\times\mathcal{Q}\mathcal{L}_{\mathrm{SB}}(\tau)\mathcal{P}\hat{W}^{(I)}(\tau)\end{aligned} \tag{2.47}$$

2.7 Time-Nonlocal Quantum Master Equation

Our starting point will be the Liouville-von Neumann equation

$$\frac{\partial}{\partial t}\hat{W}(t) = -\frac{i}{\hbar}\left[\hat{H},\hat{W}(t)\right], \tag{2.48}$$

where the Hamiltonian takes the usual form

$$\hat{H} = \hat{H}_{\mathrm{S}} + \hat{H}_{\mathrm{B}} + \hat{H}_{\mathrm{I}}, \tag{2.49}$$

where $\hat{H}_{\mathrm{S}}$ is Hamiltonian of the system, $\hat{H}_{\mathrm{B}}$ is Hamiltonian of the bath and $\hat{H}_{\mathrm{I}}$ is interaction Hamiltonian. The Hamiltonian of the whole system is transformed into an interaction picture using evolution operators of system and bath

$$\hat{H}^{(I)}(t) = \hat{U}_{\mathrm{S}}^{\dagger}(t)\hat{U}_{\mathrm{B}}^{\dagger}(t)\hat{H}\hat{U}_{\mathrm{B}}(t)\hat{U}_{\mathrm{S}}(t) \tag{2.50}$$

Transforming equation 2.48 into interaction picture and integrating for initial time $t_0 = 0$, we will obtain for $\hat{W}^{(I)}(t)$ in its integral from

$$\hat{W}^{(I)}(t) = \hat{W}^{(I)}(0) - \frac{i}{\hbar}\int_{t_0}^{t}\mathrm{d}s\left[\hat{H}_{\mathrm{I}}^{(I)}(s),\hat{W}^{(I)}(s)\right]. \tag{2.51}$$

Then we substitute this result into the right-hand side 2.48 and we will obtain the following form of Liouville-von Neumann equation

$$\begin{aligned}\frac{\partial}{\partial t}\hat{W}^{(I)}(t) =& -\frac{i}{\hbar}\left[\hat{H}_{\mathrm{I}}^{(I)}(t),\hat{W}^{(I)}(0)\right] \\ &-\frac{1}{\hbar^2}\int_{t_0}^{t}\mathrm{d}s\left[\hat{H}_{\mathrm{I}}^{(I)}(t),\left[\hat{H}_{\mathrm{I}}^{(I)}(s),\hat{W}^{(I)}(s)\right]\right].\end{aligned} \tag{2.52}$$

We should stress that no approximations are made so far in equation 2.52. A following step is to transform this equation of motion into an interaction picture of the bath. The reasoning after this step will become clear after we introduce the ansatz for a bath in the next chapter

$$\begin{aligned}\frac{\partial}{\partial t}W_{S}^{(B)}(t) =& -\frac{i}{\hbar}\left[\hat{H}_{S}(t),\hat{W}^{(B)}(t)\right] \\ &-\frac{1}{\hbar^2}\int_{t_0}^{t}\mathrm{d}s\hat{U}_{\mathrm{S}}(t)\left[\hat{H}_{\mathrm{I}}^{(I)}(t),\left[\hat{H}_{\mathrm{I}}^{(I)}(s),\hat{W}_{\mathrm{I}}^{(I)}(s)\right]\right]\hat{U}_{\mathrm{S}}^{\dagger}(t) \\ &-\frac{i}{\hbar}\hat{U}_{\mathrm{B}}^{\dagger}(t)\hat{H}_{\mathrm{I}}\hat{U}_{\mathrm{B}}(t)\hat{U}_{\mathrm{S}}(t)\hat{W}(0)\hat{U}_{\mathrm{S}}^{\dagger}(t).\end{aligned} \tag{2.53}$$

The key step of this section lies in the so-called separation of density matrix $\hat{W}(t)$ into system part $\rho_{nm}(t)$ and the bath part $\hat{w}_{nm}(t)$, that is done under the following condition

$$\rho_{nm}(t) = \mathrm{tr}_{\mathrm{B}}\left\{ \langle n|\hat{W}(t)|m\rangle \right\}, \quad \hat{w}_{nm}(t) = \frac{\langle n|\hat{W}(t)|m\rangle}{\mathrm{tr}_{\mathrm{B}}\left\{ \langle n|\hat{W}(t)|m\rangle \right\}}. \tag{2.54}$$

Therefore, this so-called separation is only done in electronic parts of the basis as shown here

$$\hat{W}(t) = \sum_{nm} \rho_{nm}(t)\hat{w}_{nm}(t)\,|n\rangle\langle m|\,, \tag{2.55}$$

and in the bath interaction picture, it is important to note that the evolution operator corresponding to the bath only acts on elements $\hat{w}_{nm}(t)$

$$\hat{W}^{(B)}(t) = \sum_{nm} \rho_{nm}(t)\hat{U}_{\mathrm{B}}^{\dagger}(t)\hat{w}_{nm}(t)\hat{U}_{\mathrm{B}}(t)\,|n\rangle\langle m|\,. \tag{2.56}$$

Now a tiny note on the properties of bath elements $\hat{w}_{nm}(t)$, the trace of these elements with respect to bath has to be equal to one

$$\begin{aligned} &\mathrm{tr}_{\mathrm{B}}\left\{\hat{w}_{nm}(t)\right\} = 1 \\ &\mathrm{tr}_{\mathrm{B}}\left\{\hat{U}_{\mathrm{B}}^{\dagger}(t)\hat{w}_{nm}(t)\hat{U}_{\mathrm{B}}(t)\right\} = 1, \end{aligned} \tag{2.57}$$

We now define the system part of matrix density in a similar fashion as it is done with projection technique 2.6

$$\hat{\rho}_{\mathrm{S}}(t) = \sum_{nm} \rho_{nm}(t)\,|n\rangle\langle m|\,. \tag{2.58}$$

Tracing out the DOF of the bath we are left with the following integrodifferential equation for system part of the density matrix

$$\begin{aligned} \frac{\partial}{\partial t}\sum_{nm}\rho_{nm}(t)\,|n\rangle\langle m| &= -\frac{i}{\hbar}\left[\hat{H}_{\mathrm{S}}, \hat{\rho}_{\mathrm{S}}(t)\right] \\ &- \frac{1}{\hbar^2}\sum_{nm}\int_{t_0}^{t}\mathrm{d}s\hat{U}_{\mathrm{S}}(t)\times \\ &\times \mathrm{tr}_{\mathrm{B}}\left\{\left[\hat{H}_{\mathrm{I}}^{(I)}(t), \left[\hat{H}_{\mathrm{I}}^{(I)}(s), \hat{U}_{\mathrm{B}}^{\dagger}(s)\hat{w}_{nm}(s)\hat{U}_{\mathrm{B}}(s)\,|n\rangle\langle m|\right]\right]\right\}\hat{U}_{\mathrm{S}}^{\dagger}(t)\rho_{nm}(s) \\ &- \frac{i}{\hbar}\sum_{nm}\mathrm{tr}_{\mathrm{B}}\left\{\hat{U}_{\mathrm{B}}^{\dagger}(t)\hat{H}_{\mathrm{I}}\hat{U}_{\mathrm{B}}(t)\hat{U}_{\mathrm{S}}(t)\hat{W}(0)\hat{U}_{\mathrm{S}}^{\dagger}(t)\right\}. \end{aligned} \tag{2.59}$$

We could consider this resulting integrodifferential equation as the prescription for system simulation, however, there is still one minor detail. In case that the bath and open quantum system are not entangled at the initial time $t_0 = 0$, following holds

$$\mathrm{tr}_{\mathrm{B}}\left\{\hat{U}_{\mathrm{B}}^{\dagger}\hat{H}_{\mathrm{I}}\hat{U}_{\mathrm{B}}\hat{W}(0)\right\} = 0. \tag{2.60}$$

Considering this extra initial condition, the last piece of the equation 2.59 disappears, and we are left with the final result

$$\begin{aligned} &\frac{\partial}{\partial t}\rho_{kl}(t) = -i\omega_{kl}\rho_{kl}(t) \\ &- \frac{1}{\hbar^2}\sum_{nm}\int_{t_0}^{t}\mathrm{d}s\,\langle k|\,\hat{U}_{\mathrm{S}}(t)\,\mathrm{tr}_{\mathrm{B}}\left\{\left[\hat{H}_{\mathrm{I}}^{(I)}(t), \left[\hat{H}_{\mathrm{I}}^{(I)}(s), \hat{U}_{\mathrm{B}}^{\dagger}(s)\hat{w}_{nm}(s)\hat{U}_{\mathrm{B}}(s)\,|n\rangle\langle m|\right]\right]\right\} \\ &\times \hat{U}_{\mathrm{S}}^{\dagger}(t)\,|l\rangle\,\rho_{nm}(s). \end{aligned}$$

(2.61)

The function under integral sign in 2.59 and 2.61 is so-called *Memory function* or *Memory kernel*

$$\begin{aligned}\mathcal{M}_{klnm}(t,s) = \\ \langle k|\,\hat{U}_{\mathrm{S}}(t)\,\mathrm{tr}_{\mathrm{B}}\left\{\left[\hat{H}_{\mathrm{I}}^{(I)}(t),\left[\hat{H}_{\mathrm{I}}^{(I)}(s),\hat{U}_{\mathrm{B}}^{\dagger}(s)\hat{w}_{nm}(s)\hat{U}_{\mathrm{B}}(s)\,|n\rangle\langle m|\right]\right]\right\}\hat{U}_{\mathrm{S}}^{\dagger}(t)\,|l\rangle\,,\end{aligned} \tag{2.62}$$

as the reader is probably expecting we can now rewrite 2.59 into the following form

$$\begin{aligned}\frac{\partial}{\partial t}\rho_{kl}(t) = -\frac{i}{\hbar}\left[\hat{H}_{\mathrm{S}},\rho_{\mathrm{S}}(t)\right] - \frac{1}{\hbar^2}\sum_{nm}\int_{t_0}^{t}\mathrm{d}s\mathcal{M}_{klmn}(t,s)\rho_{nm}(s) \\ -\frac{i}{\hbar}\sum_{nm}\mathrm{tr}_{\mathrm{B}}\left\{\hat{U}_{\mathrm{B}}^{\dagger}(t)\hat{H}_{\mathrm{I}}\hat{U}_{\mathrm{B}}(t)\hat{U}_{\mathrm{S}}(t)\hat{W}(0)\hat{U}_{\mathrm{S}}^{\dagger}(t)\right\},\end{aligned} \tag{2.63}$$

and accordingly the integrodifferential equation 2.61 into the following form

$$\begin{aligned}\frac{\partial}{\partial t}\rho_{kl}(t) = \\ -\frac{i}{\hbar}\left[\hat{H}_{\mathrm{S}},\rho_{\mathrm{S}}(t)\right] - \frac{1}{\hbar^2}\sum_{nm}\int_{t_0}^{t}\mathrm{d}s\mathcal{M}_{klmn}(t,s)\rho_{nm}(s).\end{aligned} \tag{2.64}$$

2.8 Time-Local Quantum Master Equation

In the previous section, we have derived the TNL QME, and this equation includes convolution. Solving such equation numerically is a very a challenging task. In case that the bath is infinite, we can assume that the RDM does not change significantly in the interaction picture

$$\rho^{(I)}(t-\tau) \approx \rho^{(I)}(t). \tag{2.65}$$

This assumption is also known as *Markov approximation* [May11]. Now we are allowed to rewrite time-nonlocal form of equation 2.64 into time-local form

$$\sum_{kl}\frac{\partial}{\partial t}\rho_{kl}(t)\,|k\rangle\langle l| = -\frac{i}{\hbar}\left[\hat{H}_{\mathrm{S}},\rho_{\mathrm{S}}(t)\right] + \sum_{kl}\mathcal{R}_{klnm}(t)\rho_{nm}(t)\,|k\rangle\langle l|\,. \tag{2.66}$$

The well-known Redfield equation initially derived for use in nuclear magnetic resonance [Red65], is obtained from previous equation form of QME 2.66 with integrating Redfield tensor to infinitely long timescale

$$\mathcal{R} = \lim_{t\to\infty}\mathcal{R}(t). \tag{2.67}$$

The Redfield equation has the following form

$$\sum_{kl}\frac{\partial}{\partial t}\rho_{kl}(t)\,|k\rangle\langle l| = -\frac{i}{\hbar}\left[\hat{H}_{\mathrm{S}},\rho_{\mathrm{S}}(t)\right] + \mathcal{R}_{klnm}\rho_{nm}(t)\,|k\rangle\langle l|\,. \tag{2.68}$$

This TL QME approximates the exact dynamics of the system in a weak-coupling scenario. With strong coupling, the positivity of the density matrix is broken, which leads to negative probabilities due to the numerical errors.

In our case the bath is finite, and we can express Redfield tensor in following manner

$$\mathcal{R}_{abef}(t)\rho_{ef}(t) = \int_{t_0}^{t}\mathrm{d}s\sum_{cd}\mathcal{M}_{abcd}(t,s)\mathcal{U}_{cdef}(-(t-s))\rho_{ef}(t). \tag{2.69}$$

3. Models

3.1 Monomer Hamiltonian

The building block of all systems used in this work is a monomer. It is a matter of great importance to take a closer look at monomer Hamiltonian with a purpose to gain a better understanding of underlying principles. This monomer can be in the electronic ground state and electronic excited state with energies ε_g and ε_e. Besides electron DOF the monomer also possesses vibrational DOF connected with the movement of molecule, e.g. chromophore. They are generally dependent on many coordinates, but we will replace them with one coordinate Q [May11]. As mentioned in 2.3, we restrict system only to electronic DOF. Hamiltonian has the following form

$$\hat{H} = \left(\varepsilon_g + \hat{V}_g(Q)\right) |g\rangle\langle g| + \left(\varepsilon_e + \hat{V}_e(Q)\right) |e\rangle\langle e| \,. \tag{3.1}$$

The goal will be to rewrite this Hamiltonian into a form where we can recognise system part, bath part and interaction part

$$\begin{aligned} \hat{H} &= \varepsilon_g |g\rangle\langle g| + \varepsilon_e |e\rangle\langle e| + \hat{V}_g(Q)(|g\rangle\langle g| + |e\rangle\langle e|) + \left(\hat{V}_e(Q) - \hat{V}_g(Q)\right) |e\rangle\langle e| \\ &= \varepsilon_g |g\rangle\langle g| + \varepsilon_e |e\rangle\langle e| + \hat{V}_g(Q)\mathbb{1} + \Phi(Q) |e\rangle\langle e| \\ &= \hat{H}_{\mathrm{S}} + \hat{H}_{\mathrm{B}} + \hat{H}_{\mathrm{I}}, \end{aligned} \tag{3.2}$$

where these partial Hamiltonians are defined in the following way

$$\begin{aligned} \hat{H}_{\mathrm{S}} &\equiv \varepsilon_g |g\rangle\langle g| + \varepsilon_e |e\rangle\langle e| \\ \hat{H}_{\mathrm{B}} &\equiv \hat{V}_g(Q)\mathbb{1} \\ \hat{H}_{\mathrm{I}} &\equiv \Phi(Q) |e\rangle\langle e| \,. \end{aligned} \tag{3.3}$$

An observant or skilled reader will notice that in the expanded Hamiltonian in 3.2 there seem to be many identities working on Hilbert space $\mathcal{H}_{\mathrm{B}}$, which is omitted with a purpose for better readability. We also define a practical monomer descriptor as

$$S = \frac{1}{2}\frac{d^2 m\omega}{\hbar}, \tag{3.4}$$

that is a dimensionless quantity called a *Huang-Rhys* factor; this step was done in order to reduce the number of parameters.

3.2 The Aggregate of Frenkel Excitons

The subject of study is Frenkel exciton system which was named after Yakov Frenkel [Fre31]. The Hamiltonian of such system takes the form

$$\hat{H}_{\mathrm{S}} = \sum_k \varepsilon_k |k\rangle\langle k| + \sum_{kl} J_{kl} |k\rangle\langle l| \,, \tag{3.5}$$

where states $|k\rangle$ are defined as in 2.30. Now Frenkel excitons are directly coupled through pure dephasing interaction to the bath B, which consists of a given number of harmonic oscillators. The Hamiltonian of the bath takes the form

$$\hat{H}_B = \sum_k \hat{H}_{B_k} = \sum_{k\xi_k} \frac{\hbar\omega_{\xi_k}}{2} \left(\hat{p}^2_{\xi_k} + \hat{q}^2_{\xi_k}\right), \tag{3.6}$$

and the Hamiltonian responsible for the interaction of bath and system is defined as

$$\hat{H}_I = -\hbar \sum_{k,\xi_k} \omega_{\xi_k} d_{\xi_k} \hat{q}_{\xi_k} |k\rangle\langle k| . \tag{3.7}$$

The bath is composed of individual non-interacting harmonic oscillators B_k with individual Hilbert spaces $\mathcal{H}_{\mathrm{B}_k}$. These oscillators are linked to the individual molecules of the aggregate, $\hat{q}_{\xi_k}$ is the coordinate operator of the ξ_k oscillator on the k-th molecule, ω_{ξ_k} is its assigned frequency and d_{ξ_k} is the shift of the potential energy surface of the given vibrational mode when the k-th molecule is excited, therefore in state $|e_k\rangle$. It should be noted that the shift is zero when the k-th molecule of the aggregate is in the ground state $|g_k\rangle$.

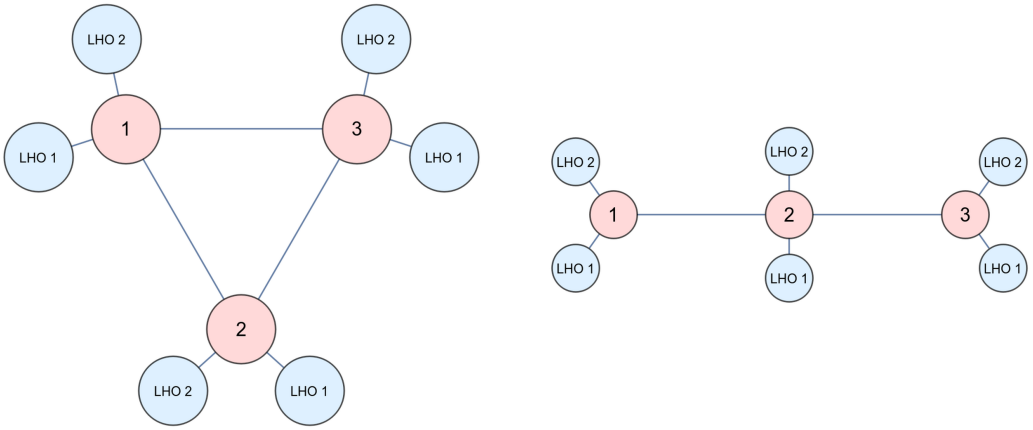

Figure 3.1: The whole system can be visualised using non-oriented graph, here we marked bath part with blue colour and system part red colour. This is only simplified version of the whole model as we do not show here the superposition of ground and excited states of excitons.

3.3 Aggregate and Bath

The more general model would contain not only the electronic and vibrational DOF of chromophores but also DOF from surrounding proteins. We split Frenkel excitons into system part and bath part, so now vibrational DOF of system excitons are still the part of system DOF. The Hamiltonian of such OQS is

defined as

$$\begin{aligned}
\hat{H}_{\mathrm{S,el}} &= \sum_{k\in I} \varepsilon_k \left|k\right\rangle\!\left\langle k\right| + \sum_{k,l\in I} J_{kl} \left|k\right\rangle\!\left\langle l\right| \\
\hat{H}_{\mathrm{S,vib}} &= \sum_{k\in I,\xi_k} \frac{\hbar\omega_{\xi_k}}{2}\left(\hat{p}^2_{\xi_k} + \hat{q}^2_{\xi_k}\right) \\
\hat{H}_{\mathrm{S,int}} &= -\hbar \sum_{k\in I,\xi_k} \omega_{\xi_k} d_{\xi_k} \hat{q}_{\xi_k} \left|k\right\rangle\!\left\langle k\right| .
\end{aligned} \tag{3.8}$$

where I is the set of electronic states corresponding to OQS. In a similar fashion we can define the bath surrounding OQS

$$\begin{aligned}
\hat{H}_{\mathrm{B,el}} &= \sum_{k\in J} \varepsilon_k \left|k\right\rangle\!\left\langle k\right| + \sum_{k,l\in J} J_{kl} \left|k\right\rangle\!\left\langle l\right| \\
\hat{H}_{\mathrm{B,vib}} &= \sum_{k\in J,\xi_k} \frac{\hbar\omega_{\xi_k}}{2}\left(\hat{p}^2_{\xi_k} + \hat{q}^2_{\xi_k}\right) \\
\hat{H}_{\mathrm{B,int}} &= -\hbar \sum_{k\in J,\xi_k} \omega_{\xi_k} d_{\xi_k} \hat{q}_{\xi_k} \left|k\right\rangle\!\left\langle k\right| ,
\end{aligned} \tag{3.9}$$

here we have a condition that $I \cup J = \{g, e_1, \ldots, e_p\}$ with p molecules in total in the whole system. With total Hamiltonian defined as

$$\begin{aligned}
H &= \hat{H}_{\mathrm{S}} + \hat{H}_{\mathrm{S}} \\
&= \hat{H}_{\mathrm{S,el}} + \hat{H}_{\mathrm{S,vib}} + \hat{H}_{\mathrm{S,int}} + \hat{H}_{\mathrm{B,el}} + \hat{H}_{\mathrm{B,vib}} + \hat{H}_{\mathrm{B,int}}
\end{aligned} \tag{3.10}$$

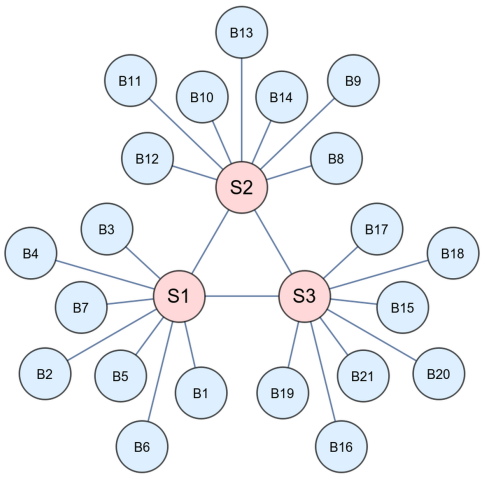

Figure 3.2: Another example of representation with a non-oriented graph for general OQS with more general bath.

4. Derived Theory

4.1 The Ansatz for the Bath

In the section where TNL QME is derived 2.7, the total density matrix $\hat{W}(t)$ is separated between two part. The RDM $\hat{\rho}(t)$ and the bath part $\hat{w}(t)$. The advantage of this separation is that now, we can introduce ansatz for $\hat{w}(t)$. The bath part of density matrix is part of memory kernel, that can be calculated exactly if needed. Using evolution superoperators of Liouville equation we can calculate $\hat{W}(t)$ to desired precision. Consequently $\hat{w}(t)$ can be calculated as in 2.54 for $t > t_0$ with $\mathcal{M}_{abcd}(t, s)$.

The pivoting point of this work is the formulation of the ansatz for the bath. The assumption is that the bath part of density matrix is constant

$$\hat{w}_{cd} = \hat{w}_{cd}(t), \quad t \geq t_0, \tag{4.1}$$

again $\mathcal{M}_{abcd}(t, s)$ can be calculated and compared to the exact memory kernel. We should stress that the ansatz is made with respect to the site basis and not to the exciton basis.

4.2 Memory Kernel of the First Kind

The previous section contains a prescription on how to evaluate the memory kernel $\mathcal{M}(t, s)$, see 2.62. Dependency on two time variables can be uncomfortable from a purely practical point of view. With scaling the system bath or adding more molecules to the aggregate, the basis of the total system grows exponentially. Even if the initial condition is pure state, it would be difficult to obtain reasonable numerical results for larger systems. We are motivated to find time dependence of memory kernel only on one time variable. Let us begin with the same memory kernel, but before applying trace over bath from 2.53, so we start with the expression

$$\begin{aligned}&\mathcal{M}'(t, t-s)\hat{W}(t-s) = \\ &\quad \hat{U}_{\mathrm{S}}(t)\left[\hat{H}_{\mathrm{I}}^{(I)}(t), \left[\hat{H}_{\mathrm{I}}^{(I)}(s), \hat{U}_{\mathrm{SB}}^{\dagger}(t-s)\hat{W}(t-s)\hat{U}_{\mathrm{SB}}(t-s)\right]\right]\hat{U}_{\mathrm{S}}^{\dagger}(t)\end{aligned} \tag{4.2}$$

and again using expansion of Hamiltonian in the inner commutator we get

$$\begin{aligned}&\mathcal{M}'(t, t-s)\hat{W}(t-s) = \\ &\quad \hat{U}_{\mathrm{S}}(t)\left[\hat{U}_{\mathrm{SB}}^{\dagger}(t)\hat{H}_{\mathrm{I}}\hat{U}_{\mathrm{SB}}(t), \hat{U}_{\mathrm{SB}}^{\dagger}(t-s)\hat{H}_{\mathrm{I}}\hat{W}(t-s)\hat{U}_{\mathrm{SB}}(t-s)\right]\hat{U}_{\mathrm{S}}^{\dagger}(t) \\ &-\hat{U}_{\mathrm{S}}(t)\left[\hat{U}_{\mathrm{SB}}^{\dagger}(t)\hat{H}_{\mathrm{I}}\hat{U}_{\mathrm{SB}}^{\dagger}(t), \hat{U}_{\mathrm{SB}}^{\dagger}(t-s)\hat{W}(t-s)\hat{H}_{\mathrm{I}}\hat{U}_{\mathrm{SB}}^{\dagger}(t-s)\right]\hat{U}_{\mathrm{S}}^{\dagger}(t).\end{aligned} \tag{4.3}$$

With another rearrangement of evolution operators we will obtain the final form

$$\begin{aligned}&\mathcal{M}'(t, t-s)\hat{W}(t-s) = \\ &\quad \hat{U}_{\mathrm{B}}(t)\Big(\left[\hat{H}_{\mathrm{I}}, \hat{U}_{\mathrm{SB}}^{\dagger}(-s)\hat{H}_{\mathrm{I}}\hat{W}(t-s)\hat{U}_{\mathrm{SB}}(-s)\right] \\ &\qquad -\left[\hat{H}_{\mathrm{I}}, \hat{U}_{\mathrm{SB}}^{\dagger}(-s)\hat{W}(t-s)\hat{H}_{\mathrm{I}}\hat{U}_{\mathrm{SB}}^{\dagger}(-s)\right]\Big)\hat{U}_{\mathrm{B}}^{\dagger}(t),\end{aligned} \tag{4.4}$$

and we rewrite the stated memory kernel, so that it is dependent only on one time variable

$$\mathcal{M}'(t, t-s) = \hat{U}_{\mathrm{B}}(t)\mathcal{M}(t-s)\hat{U}_{\mathrm{B}}^{\dagger}(t) \tag{4.5}$$

Key step is to rewrite the traced integral with the memory kernel to more computationally favourable way

$$\begin{aligned}
&\int_{t_0}^{t} \mathrm{d}s\, \hat{U}_{\mathrm{S}}(t)\, \mathrm{tr}_{\mathrm{B}} \left\{ \left[\hat{H}_{\mathrm{I}}^{(I)}(t), \left[\hat{H}_{\mathrm{I}}^{(I)}(s), \hat{W}_{\mathrm{I}}(s) \right] \right] \right\} \hat{U}_{\mathrm{S}}^{\dagger}(t) = \\
&\qquad = \mathrm{tr}_{\mathrm{B}} \left\{ \int_{0}^{t-t_0} \mathrm{d}s\, \hat{U}_{\mathrm{S}}(t) \left[\hat{H}_{\mathrm{I}}^{(I)}(t), \left[\hat{H}_{\mathrm{I}}^{(I)}(t-s), \hat{W}_{\mathrm{I}}(t-s) \right] \right] \hat{U}_{\mathrm{S}}^{\dagger}(t) \right\} \\
&\qquad = \mathrm{tr}_{\mathrm{B}} \left\{ \hat{U}_{\mathrm{B}}(t) \Big(\int_{0}^{t-t_0} \mathrm{d}s\, \mathcal{M}(t-s)\hat{W}(t-s) \Big) \hat{U}_{\mathrm{B}}^{\dagger}(t) \right\}.
\end{aligned} \tag{4.6}$$

In the last part of this section, we will state explicitly the structure of memory kernel $\mathcal{M}(t)$, that is, the following form

$$\mathcal{M}(t)\hat{W} = \hat{M}_1\hat{W}\hat{M}_2 - \hat{M}_3\hat{W}\hat{M}_4 - \hat{M}_5\hat{W}\hat{M}_6 + \hat{M}_7\hat{W}\hat{M}_8, \tag{4.7}$$

with operators M_i defined in the following way

$$\begin{array}{ll}
M_1(t) = \hat{H}_{\mathrm{I}}\hat{U}_{\mathrm{SB}}^{\dagger}(-t)\hat{H}_{\mathrm{I}} & M_2(t) = \hat{U}_{\mathrm{SB}}(-t) \\
M_3(t) = \hat{U}_{\mathrm{SB}}^{\dagger}(-t)\hat{H}_{\mathrm{I}} & M_4(t) = \hat{U}_{\mathrm{SB}}(-t)\hat{H}_{\mathrm{I}} \\
M_5(t) = \hat{H}_{\mathrm{I}}\hat{U}_{\mathrm{SB}}^{\dagger}(-t) & M_6(t) = \hat{H}_{\mathrm{I}}\hat{U}_{\mathrm{SB}}(-t) \\
M_7(t) = \hat{U}_{\mathrm{SB}}^{\dagger} & M_8(t) = \hat{H}_{\mathrm{I}}\hat{U}_{\mathrm{SB}}(-t)\hat{H}_{\mathrm{I}},
\end{array} \tag{4.8}$$

again, this explicit notation of $\hat{M}_i$ is only necessary in order to perform simulations efficiently. We will stress that derived form of kernel is suitable only for dynamics in the interaction picture of bath with ansatz defined in 2.55.

4.3 Memory Kernel of the Second Kind

More promising is a different approach, we start as in previous section with Liouville-von Neumann equation for RDM, but in the interaction picture of the system and the bath

$$\begin{aligned}
&\frac{\partial}{\partial t}\rho^{(I)}(t) = -\frac{i}{\hbar}\, \mathrm{tr}_{\mathrm{B}} \left\{ \left[\hat{H}_{\mathrm{I}}^{(I)}(t), \hat{W}^{(I)}(0) \right] \right\} - \frac{1}{\hbar^2} \int_{t_0}^{t} \mathrm{d}s\, \mathcal{M}(t,s)\hat{W}^{(I)}(s) \\
&\mathcal{M}(t,s)\hat{W}(s) = \mathrm{tr}_{\mathrm{B}} \left[\hat{H}_{\mathrm{I}}^{(I)}(t), \left[\hat{H}_{\mathrm{I}}^{(I)}(s), \hat{W}^{(I)}(s) \right] \right].
\end{aligned} \tag{4.9}$$

Our motivation is to expand the compact notation of Memory kernel in 4.9 so that RDM elements in the interaction picture can be obtained. The first step will consist of expanding commutators inside the trace

$$\begin{aligned}
\mathcal{M}(t,s)\hat{W}(s) = &+ \mathrm{tr}_{\mathrm{B}} \left\{ \hat{H}_{\mathrm{I}}^{(I)}(t)\hat{H}_{\mathrm{I}}^{(I)}(s)\hat{W}_{\mathrm{I}}^{(I)}(s) \right\} \\
&- \mathrm{tr}_{\mathrm{B}} \left\{ \hat{H}_{\mathrm{I}}^{(I)}(t)\hat{W}_{\mathrm{I}}^{(I)}(s)\hat{H}_{\mathrm{I}}^{(I)}(s) \right\} \\
&- \mathrm{tr}_{\mathrm{B}} \left\{ \hat{H}_{\mathrm{I}}^{(I)}(s)\hat{W}_{\mathrm{I}}^{(I)}(s)\hat{H}_{\mathrm{I}}^{(I)}(t) \right\} \\
&+ \mathrm{tr}_{\mathrm{B}} \left\{ \hat{W}_{\mathrm{I}}^{(I)}(s)\hat{H}_{\mathrm{I}}^{(I)}(s)\hat{H}_{\mathrm{I}}^{(I)}(t) \right\} \\
\mathcal{M}(t,s)\hat{W}(s) = &\mathcal{M}_1(t,s)\hat{W}(s) - \mathcal{M}_2(t,s)\hat{W}(s) - \mathcal{M}_3(t,s)\hat{W}(s) + \mathcal{M}_4(t,s)\hat{W}(s),
\end{aligned}$$

(4.10)

where each part of a memory kernel will be expanded in the following part of this section. We can realize that there is a neat property linking two pairs of the memory kernel parts

$$\begin{aligned}
&\left(\mathcal{M}_1(t,s)\hat{W}(s)\right)^\dagger = \\
&\quad = \left(\mathrm{tr}_\mathrm{B}\left\{\hat{H}_\mathrm{I}^{(I)}(t)\hat{H}_\mathrm{I}^{(I)}(s)\hat{W}_\mathrm{I}^{(I)}(s)\right\}\right)^\dagger \\
&\quad = \mathrm{tr}_\mathrm{B}\left\{\hat{W}_\mathrm{I}^{(I)}(s)\hat{H}_\mathrm{I}^{(I)}(s)\hat{H}_\mathrm{I}^{(I)}(t)\right\} \\
&\quad = \mathcal{M}_4(t,s)\hat{W}(s),
\end{aligned} \tag{4.11}$$

hence we can rewrite 4.10 to a more compact version and we are left with evaluating only two parts of the memory function

$$\mathcal{M}(t,s)\hat{W}(s) = \mathcal{M}_1(t,s)\hat{W}(s) + \mathrm{h.c.} + \mathcal{M}_2(t,s)\hat{W}(s) + \mathrm{h.c.}. \tag{4.12}$$

For better readability, we will rewrite all Hamiltonians and density matrix in $\mathcal{M}_1(t,s)\hat{W}(s)$ back to Schrodinger picture

$$\begin{aligned}
&\mathcal{M}_1(t,s)\hat{W}(s) = \\
&\quad = \mathrm{tr}_\mathrm{B}\Big\{\hat{U}_\mathrm{S}^\dagger(t)\hat{U}_\mathrm{B}^\dagger(t)\hat{H}_\mathrm{I}\hat{U}_\mathrm{B}(t)\hat{U}_\mathrm{S}(t)\ \hat{U}_\mathrm{S}^\dagger(s)\hat{U}_\mathrm{B}^\dagger(s)\hat{H}_\mathrm{I}\hat{U}_\mathrm{B}(s)\hat{U}_\mathrm{S}(s) \\
&\qquad \hat{U}_\mathrm{S}^\dagger(s)\hat{U}_\mathrm{B}^\dagger(s)\hat{W}(s)\hat{U}_\mathrm{B}(s)\hat{U}_\mathrm{S}(s)\Big\} \\
&\quad = \mathrm{tr}_\mathrm{B}\left\{\hat{U}_\mathrm{S}^\dagger(t)\hat{H}_\mathrm{I}\hat{U}_\mathrm{B}(t-s)\hat{U}_\mathrm{S}(t-s)\hat{H}_\mathrm{I}\hat{U}_\mathrm{S}(s)\hat{W}^{(S)}(s)\hat{U}_\mathrm{B}^\dagger(t-s)\right\} \\
&\quad = \hat{U}_\mathrm{S}^\dagger(t)\,\mathrm{tr}_\mathrm{B}\left\{\hat{U}_\mathrm{B}^\dagger(t-s)\hat{H}_\mathrm{I}\hat{U}_\mathrm{B}(t-s)\hat{U}_\mathrm{S}(t-s)\hat{H}_\mathrm{I}\hat{U}_\mathrm{S}(s)\hat{W}^{(S)}(s)\right\},
\end{aligned} \tag{4.13}$$

where the cyclic property of the trace was used at the last line. Similar can be done in the second part of memory function multiplied by density matrix in the interaction picture $\mathcal{M}_2(t,s)W(s)$

$$\begin{aligned}
&\mathcal{M}_2(t,s)\hat{W}(s) = \\
&\quad = \mathrm{tr}_\mathrm{B}\Big\{\hat{U}^a t U_\mathrm{S}^\dagger(t)\hat{U}_\mathrm{B}^\dagger(t)\hat{H}_\mathrm{I}\hat{U}_\mathrm{B}(t)\hat{U}_\mathrm{S}(t)\ \hat{U}_\mathrm{S}^\dagger(s)\hat{U}_\mathrm{B}^\dagger(s)\hat{W}(s)\hat{U}_\mathrm{B}(s)\hat{U}_\mathrm{S}(s) \\
&\qquad \hat{U}_\mathrm{S}^\dagger(s)\hat{U}_\mathrm{B}^\dagger(s)\hat{H}_\mathrm{I}\hat{U}_\mathrm{B}(s)\hat{U}_\mathrm{S}(s)\Big\} \\
&\quad = \mathrm{tr}_\mathrm{B}\left\{\hat{U}_\mathrm{S}^\dagger(t-s)\hat{H}_\mathrm{I}\hat{U}_\mathrm{B}(t-s)\hat{U}_\mathrm{S}(t)\hat{W}^{(S)}(s)\hat{U}_\mathrm{S}^\dagger(s)\hat{H}_\mathrm{I}\hat{U}_\mathrm{B}^\dagger(t-s)\right\} \\
&\quad = \hat{U}_\mathrm{S}^\dagger(s)\,\mathrm{tr}_\mathrm{B}\left\{\hat{H}_\mathrm{I}\hat{U}_\mathrm{B}^\dagger(t-s)\hat{U}_\mathrm{S}^\dagger(t-s)\hat{H}_\mathrm{I}\hat{U}_\mathrm{B}(t-s)\hat{U}_\mathrm{S}(t)\hat{W}^{(S)}(s)\right\},
\end{aligned} \tag{4.14}$$

where we again used the fact that $\hat{U}_\mathrm{S}$ and $\hat{U}_\mathrm{B}$ are in fact operating on different Hilbert spaces and the cyclicity of the trace operation. We will proceed by expressing matrix values of $\langle a|\mathcal{M}_i(t,s)W(s)|b\rangle$

$$\begin{aligned}
&\langle a|\mathcal{M}_1(t,s)\hat{W}(s)|b\rangle = \\
&\quad = \langle a|\,\hat{U}_\mathrm{S}^\dagger(t)\,\mathrm{tr}_\mathrm{B}\left\{\hat{U}_\mathrm{B}^\dagger(t-s)\hat{H}_\mathrm{I}\hat{U}_\mathrm{B}(t-s)\hat{U}_\mathrm{S}(t-s)\hat{H}_\mathrm{I}\hat{U}_\mathrm{S}(s)\hat{W}^{(S)}(s)\right\}|b\rangle \\
&\quad = \sum_{nm} e^{\frac{i}{\hbar}\varepsilon_a t}e^{-\frac{i}{\hbar}\varepsilon_k(t-s)}e^{-\frac{i}{\hbar}\varepsilon_n s}\times \\
&\qquad \times \mathrm{tr}_\mathrm{B}\Big\{\langle a|\,\hat{U}_\mathrm{B}^\dagger(t-s)\hat{H}_\mathrm{I}\hat{U}_\mathrm{B}(t-s)\hat{H}_\mathrm{I}\,|n\rangle\,\hat{w}_{nm}(s)\,\langle m|b\rangle\Big\}\rho_{nm}^{(I)}(s),
\end{aligned} \tag{4.15}$$

here we assumed that the $\hat{H}_{\mathrm{S}}$ is diagonal in the electronic basis. In the next step, we will use the orthogonality of excitonic states and the substitution $\omega_{ab} = (\varepsilon_a - \varepsilon_b)/\hbar$. Let us proceed further with expressing operator multiplication inside the trace in terms of electronic states

$$\begin{aligned}\langle a|\mathcal{M}_1(t,s)\hat{W}(s)|b\rangle &= \\ &= \sum_{nm} e^{i\omega_{ak}t} e^{i\omega_{kn}s} \times \\ &\quad \times \mathrm{tr}_{\mathrm{B}} \left\{ \hat{U}_{\mathrm{B}}^{\dagger}(t-s)\, \langle a|\hat{H}_{\mathrm{I}}|k\rangle\, \hat{U}_{\mathrm{B}}(t-s)\, \langle k|\hat{H}_{\mathrm{I}}|n\rangle\, \hat{w}_{nb}(s) \right\} \rho_{nb}^{(I)}(s).\end{aligned} \tag{4.16}$$

Similar steps can be performed with the purpose of finding $\langle a|\hat{H}_{\mathrm{I}}|b\rangle$ elements. We assume that the interaction Hamiltonian can be written in terms of some states $|\alpha\rangle$

$$\hat{H}_{\mathrm{I}} = \sum_{\alpha} \Delta\hat{V}_{\alpha}\, |\alpha\rangle\langle\alpha| \,. \tag{4.17}$$

Now we need to express this interaction Hamiltonian in terms of our electronic basis

$$\begin{aligned}\hat{H}_{\mathrm{I}} &= \sum_{ab} |a\rangle\langle a| \sum_{\alpha} \Delta\hat{V}_{\alpha}\, |\alpha\rangle\langle\alpha|\, |b\rangle\langle b| \\ &= \sum_{ab} \left(\sum_{\alpha} \Delta\hat{V}_{\alpha}\, \langle a|\alpha\rangle\, \langle\alpha|b\rangle \right) |a\rangle\langle b| \\ &= \sum_{ab} \Delta\hat{V}_{ab}\, |a\rangle\langle b| \,.\end{aligned} \tag{4.18}$$

This established notation with separated interaction Hamiltonian can be plugged back into 4.16 so we will obtain

$$\begin{aligned}\langle a|\mathcal{M}_1(t,s)\hat{W}(s)|b\rangle &= \sum_{nk} e^{i\omega_{ak}t} e^{i\omega_{kn}s} \times \\ &\quad \times \mathrm{tr}_{\mathrm{B}} \left\{ \hat{U}_{\mathrm{B}}^{\dagger}(t-s) \Delta\hat{V}_{ak} \hat{U}_{\mathrm{B}}(t-s) \Delta\hat{V}_{kn} \hat{w}nb(s) \right\} \rho_{nb}^{(I)}(s).\end{aligned} \tag{4.19}$$

The exact same procedure can be applied in the last line in the equation 4.14, we will get following expression

$$\begin{aligned}\langle a|\mathcal{M}_2(t,s)\hat{W}(s)|b\rangle &= \sum_{nk} e^{i\omega_{kn}t} e^{i\omega_{ak}s} \\ &\quad \times \mathrm{tr}_{\mathrm{B}} \left\{ \Delta\hat{V}_{ak} \hat{U}_{\mathrm{B}}^{\dagger}(t-s) \Delta\hat{V}_{kn} \hat{U}_{\mathrm{B}}(t-s) \hat{w}nb(s) \right\} \rho_{nb}^{(I)}(s).\end{aligned} \tag{4.20}$$

5. Numerical Results

5.1 Initial Condition

Throughout this work, we have two different ways how to set the initial condition. In the first approach, we will set an initial condition that is restricted and artificial, in a way that this sort of condition will not be possible to reconstruct in an experiment. However, it may be beneficial to fulfil our aspiration to inspect some specific aspects of the system.

This specific initial condition can, for an example, have the following form

$$|\psi(0)\rangle = |\xi^0_{e_1}\rangle|\xi^0_{g_2}\rangle \dots |\xi^0_{g_p}\rangle, \tag{5.1}$$

here the only first electronic state is populated with all LHOs only in the lowest vibrational state. We could be interested in the condition that sets gaussian wave-packet into the ground or excited state of a specific molecule in the aggregate.

$$|n(q)\rangle = \frac{1}{\sqrt{2^n n!}} \left(\frac{m\omega}{\pi\hbar}\right)^{1/4} H_n\left(\sqrt{\frac{m\omega}{\hbar}}q\right) \exp\left(-\frac{m\omega q^2}{2\hbar}\right), \tag{5.2}$$

here it is worth mentioning that we usually put $m = \hbar = 1$. Nevertheless, with given distribution, in our case normal distribution

$$f(q, \sigma, \mu) = \frac{1}{\sigma\sqrt{2\pi}} \exp\left[-\frac{1}{2}\left(\frac{q-\mu}{\sigma}\right)^2\right], \tag{5.3}$$

we are in a position to find corresponding weights with Fourier transform to construct

$$|\psi_k\rangle = \sum_{i=1}^{N} w_{ki}|\xi^i_{a_k}\rangle, \tag{5.4}$$

where $a_k \in \{g_k, e_k\}$ and the total wave-function is after this procedure constructed as

$$|\psi\rangle = \prod_{k=1}^{p} |\psi_k\rangle\,. \tag{5.5}$$

There is one minor detail worth mentioning for readers that consider using the previous condition. Because we are always working in a finite basis, it is indisputably crucial to normalise state-vector $|\psi_k\rangle$. This obtained state is pure as we only have $W = |\psi\rangle\langle\psi|$.

The other sort of the initial condition is essential for simulating possible experiments. The first step is to find the density matrix at the equilibrium W_{eq} using 2.33. After this step, we will simulate laser excitation. With excitation, we use two kinds of excitation operator $\hat{\mu}$, which is symmetric and not symmetric. Matrix elements of the symmetric excitation operator $\hat{\mu}_{\text{sym}}$ are defined in electronic basis in the following way

$$\mu_{\text{sym},nm} = \begin{cases} \mu_0 & n = 1,\ m \geq 2 \text{ or } n \geq 2,\ m = 1 \\ 0 & \text{otherwise,} \end{cases} \tag{5.6}$$

for non-symmetric excitation operator $\hat{\mu}_k$ we have the following definition

$$\mu_{k,nm} = \begin{cases} \mu_0 & n = 1,\ m = k \text{ or } n = k,\ m = 1 \\ 0 & \text{otherwise.} \end{cases} \tag{5.7}$$

We would like to stress again that we work only with one-excited states. The laser field intensity E_0 and dipole moment amplitude μ_0 are chosen to be

$$E_0\mu_0 = 1.5\,\mathrm{cm}^{-1}\mathrm{fs}\ . \tag{5.8}$$

This sort of initial condition is a mixed state with a growing system basis; it is gradually more challenging to perform numerical simulations with the whole density matrix $\hat{W}(t)$. There is a way to overcome this difficulty, that being said, every mixed state $\hat{W}$ can be decomposed into pure states $|\psi_i\rangle\langle\psi_i|$ with weights w_i. However, this decomposition is not unique, and in fact, there seem to be infinitely many possible decompositions of such state. This can be valuable in finding a minimum number of pure states to satisfy specific precision criteria for reconstruction of $\hat{W}$. As a result, pure states can be used with the Schrödinger equation to give more precise numerical results as we can afford adaptive step methods to solve ODEs. More on mixed state decomposition in the appendix A.2.

5.2 Methods on Solving Differential Equations

In this work, we used mainly three types of solving techniques. In this section, we will discuss technical aspects which are unavoidable for reproducing results in this work. However, a reader who is only interested in numerical results and conclusions can skip the rest of this section.

The first class of the problem is to evaluate wave-function $|\psi(t)\rangle$ on the interval $t \in (t_0, t_1)$ with the Schrödinger equation

$$\frac{d}{dt}\,|\psi(t)\rangle = -\frac{i}{\hbar}\hat{H}\,|\psi(t)\rangle\,, \tag{5.9}$$

this is, in fact, well-posted ODE problem. We selected *julia* as a language capable of both outstanding performance and strong community support. The package *DifferentialEquations.jl* [RN17] contains plenty of ODE solvers, we choose Verner's "Most Efficient" 9/8 Runge-Kutta method [Nak58] with adaptive stepsize. The tolerances were set to rtol $= 10^{-8}$ and atol $= 10^{-8}$ for the basis size under thousand elements. In the case of a bigger size of basis, we tighten the tolerances so that the fluctuations of the total energy of the system are negligible. In case that we have an initial condition in the form of mixed state we can decompose it into the set of pure states to meet some precision criterion $W(0) = \sum_i |\psi_i(0)\rangle\langle\psi_i(0)|$ and similarly, we solve $|\psi_i(t)\rangle$ on defined timescale; in some cases, this approach can be more effective overall. In case that we are working in the locally orthogonal basis, it is preferable to choose sparse matrices for Hamiltonian representation.

The second class of the problem is to find a density matrix of the system $\hat{W}(t)$ on a well-defined interval using evolution operators

$$\hat{W}(t) = \mathcal{U}(t)\hat{W}(0) = \hat{U}(t)\hat{W}(0)\hat{U}^{\dagger}(t) = e^{-\frac{i}{\hbar}\hat{H}t}\hat{W}(0)e^{\frac{i}{\hbar}\hat{H}t}. \tag{5.10}$$

The difficulty of this task lies in evaluating these exponentials. In most cases there seem to be no shortcuts, but depending on the size of basis and sparsity of Hamiltonian, the reader should also consider diagonalisation.

The last class of the problem is the most challenging; in this work, we are dealing with ansatz and altered Quantum Master Equations. In general, we want to solve following integrodifferential equation

$$\frac{\partial}{\partial t}\hat{W}(t) = \mathcal{K}(t)\hat{W}(t) + \int_{t_0}^{t} \mathrm{d}s\mathcal{M}(t,s)\hat{W}(s), \tag{5.11}$$

here we usually evaluate $\mathcal{K}(t)$ and $\mathcal{M}(t,s)$ beforehand, we are limited to a relatively small number of steps $N \in (200, 1000)$ and we usually can not afford to use Runge-Kutta of 4th order.

5.3 On the Difficulty of Numerical Simulations

The ultimate difficulty, which prevents us from simulating irreversible systems, is the exponential growth of basis. In this section, we will demonstrate how quickly is this problem becoming unsolvable. Before the main simulations were carried out in this work, the author was focused on the efficient calculation of Franck-Condon factors for a limited number of elements of vibrational basis. Calculation of Franck-Condon factors is the most CPU-intensive task during the evaluation of Hamiltonian elements.

In order to obtain any meaningful information from calculated wave-function $|\psi(t)\rangle$ we have to perform the trace over the bath degrees of freedom. Without the use of the product of Franck-Condon factors, this operation quickly becomes the most CPU-intensive task in the whole simulation. For the given simulation, this product can be calculated beforehand and applied after the simulation. The author applied this method in the Python package *quantarhei* freely available on Github, which is still sufficient for the relatively modest size of basis. Due to the sparsity of Franck-Condon factors, some optimisations can be done on the numerical side of the problem, more on that in the appendices A.1, A.3 and A.4.

The last and the most concerning problem is the solution of ODE, which represents the Schrödinger equation as mentioned in the previous section. We use Verner's "Most Efficient" 9/8 Runge-Kutta method, which we consider as the best option due to the high precision to CPU cost value for high-dimensional systems. This method uses adaptive step-size, which we strongly recommend for the reader interested in a similar type of simulation.

Several simulations were carried out with the dimer model and trimer model at the same machine using processor *Intel Core i5-9300H* without a turbo boost working at 2.4 GHz. Timescale was set to $t \in (0, 100)$ $(a.u.)$ with precision rtol $= 10^{-8}$ and atol $= 10^{-8}$, also the total density matrix was traced at one thousand different time values. In the graph 5.1 we can observe the cost of the Hamiltonian evaluation, Franck-Condon product calculation and the cost of dynamics together with a trace operation.

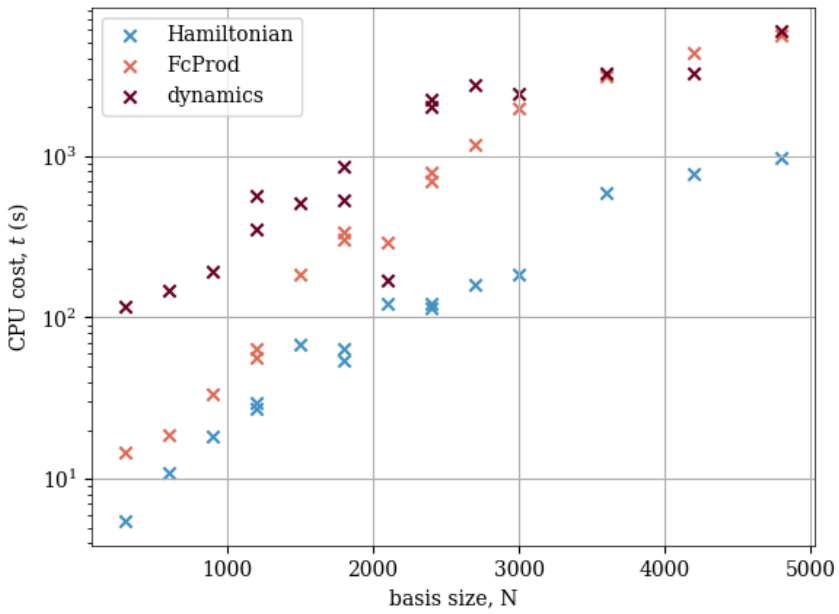

Figure 5.1: For the total system basis Hamiltonian evaluation, Franck-Condon factors product calculation and the overall dynamics were performed. The CPU time used to perform each of these tasks is here shown as the function of the basis size.

5.4 Methods of Exact the Numerical Solution

To discuss numerical results obtained from QME using the ansatz 4.1 we have to compare these results to the exact dynamics. Exact dynamics can be obtained with evolution operators of the whole system $\hat{U}(t)$ acting on the initial density matrix $\hat{W}(t)$

$$\rho(t) = \mathrm{tr}_\mathrm{B}\left\{\hat{U}(t)W_0\hat{U}^\dagger(t)\right\}. \tag{5.12}$$

The other approach is based on using QME in the following form

$$\begin{aligned}\frac{\partial}{\partial t}\hat{W}^{(I)}(t) &= \\ &= -\frac{i}{\hbar}\left[H_\mathrm{I}^{(I)}(t), \hat{W}^{(I)}(t)\right] - \frac{1}{\hbar^2}\int_{t_0}^{t}\mathrm{d}s\left[\hat{H}_\mathrm{I}^{(I)}(t), \left[\hat{H}_\mathrm{I}^{(I)}(s), \hat{W}^{(I)}(s)\right]\right] \\ \rho(t) &= \hat{U}_\mathrm{S}(t)\,\mathrm{tr}_\mathrm{B}\left\{\hat{W}^{(I)}(t)\right\}\hat{U}_\mathrm{S}^\dagger(t).\end{aligned} \tag{5.13}$$

There is great importance in comparing both recipes. Solving IDE is a delicate task concerning the numerical stability of the solution. The ideal scenario would be using adaptive step-size with delayed differential equation solvers and some standard method, e.g. RK4. Evaluating memory kernel with respect to two time variables t, s is a CPU-intensive task for a reasonable size of vibrational basis, even using *julia* language and corresponding libraries. The amortised time complexity of these calculations has a quadratic dependency on the number of time steps $O(N_\mathrm{steps}^2)$.

5.5 The Limit Case of Weak Bath Interaction

To verify the usefulness of the ansatz, we have to inspect the case where the bath interaction as a result vanishes. That means we have to inspect the response of the simulated system to the Huang-Rhys parameter. This parameter is usually set to the value $S = 0.05$ in our case. In this section, we will test the response for these values $S \in \{0.05, 0.025, 0.0125, 0.00625, 0\}$. Numerical simulations for the system with ansatz for the bath 4.1 were carried out and compared to the exact dynamics using evolution operators 5.12 and Liouville von Neumann equation 2.16. For a model, we choose dimer with one LHO coupled with each molecule, and the frequencies are set to $\omega_{1,2} = 100\,\mathrm{cm}^{-1}$. Energies of the molecules are $E_1 = 12500\,\mathrm{cm}^{-1}$ and $E_2 = 12400\,\mathrm{cm}^{-1}$. The coupling in system Hamiltonian is set to $J = 100\,\mathrm{cm}^{-1}$. The initial condition was set as a pure state created by laser excitation from the ground electronic and vibrational state in site basis.

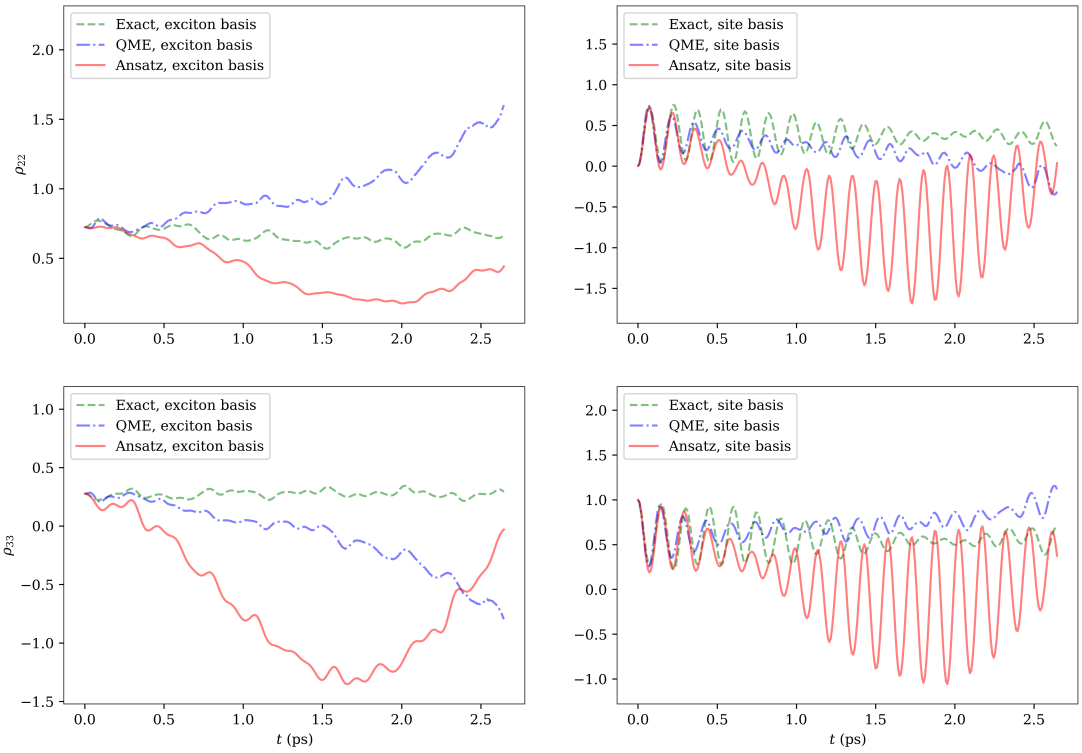

Figure 5.2: Compared dynamics of the exact solution with evolution operators (green, dashed), exact TNL QME (blue, dashdotted) and the ansatz for the bath using TNL QME (red, full). The Huang-Rhys factor in the interaction Hamiltonian was set to $S = 0.05$.

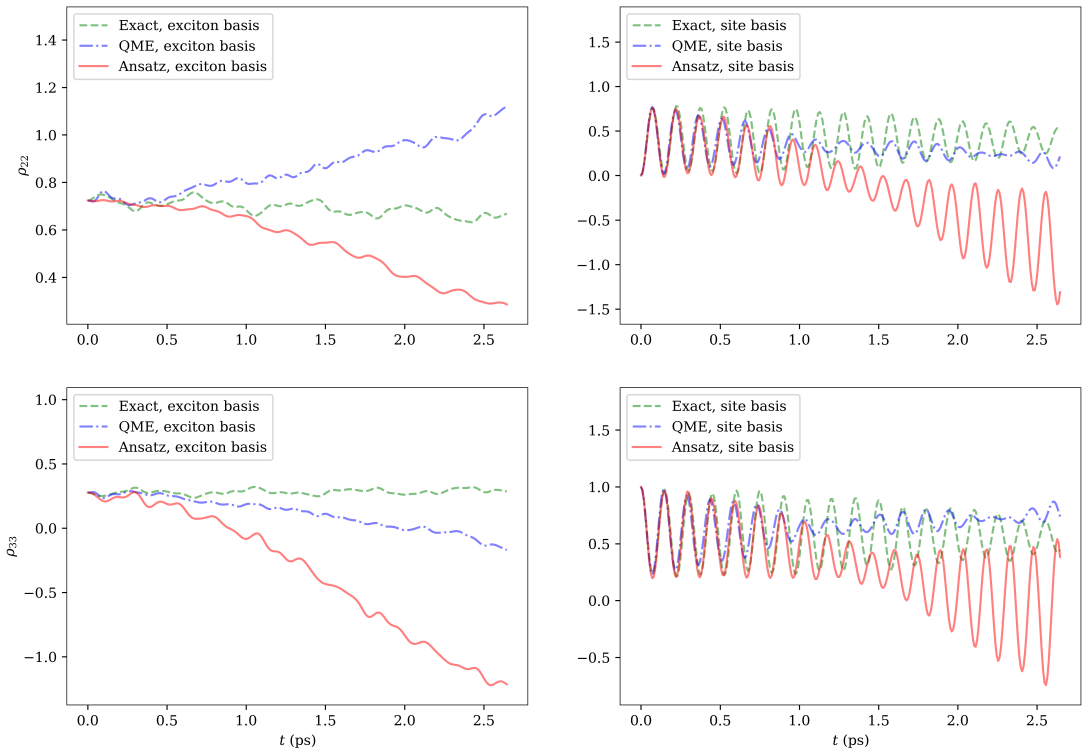

Figure 5.3: The Huang-Rhys factor in the interaction Hamiltonian was set to $S = 0.025$.

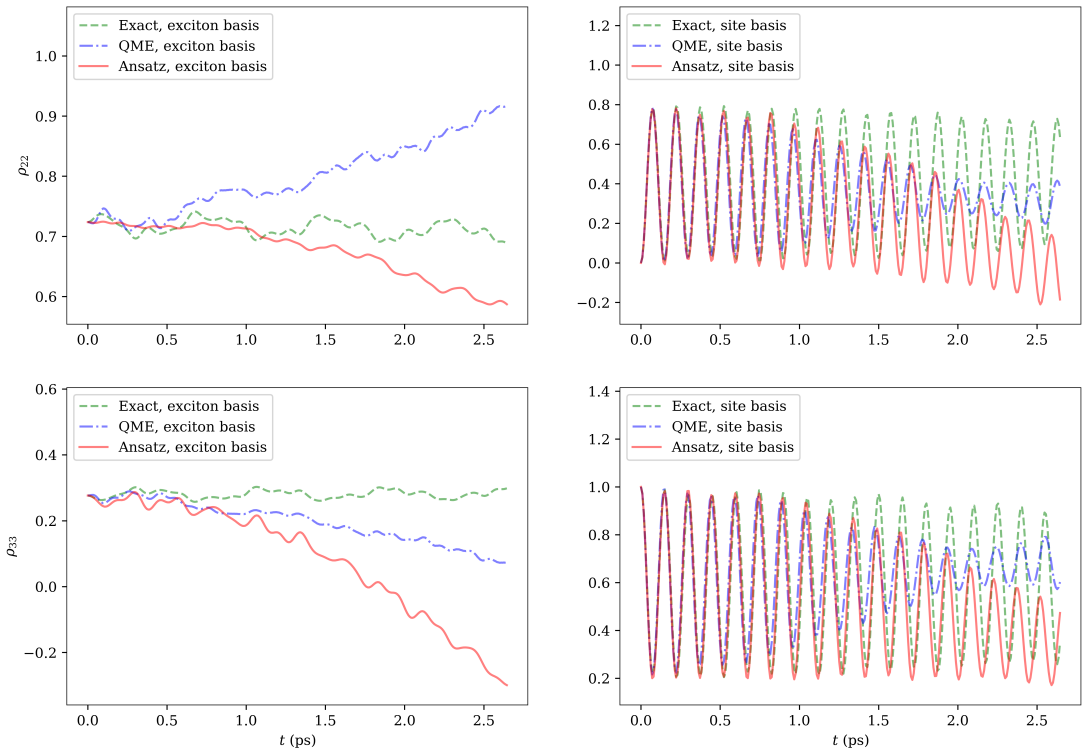

Figure 5.4: The Huang-Rhys factor in the interaction Hamiltonian was set to $S = 0.0125$.

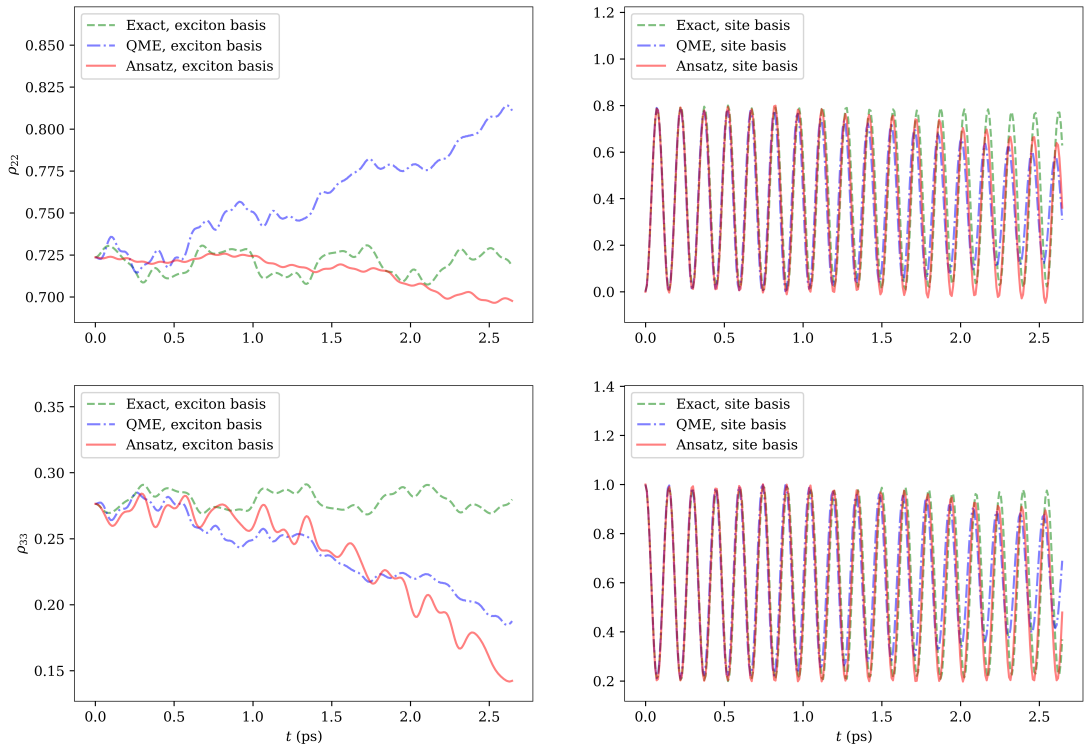

Figure 5.5: The Huang-Rhys factor in the interaction Hamiltonian was set to $S = 0.00625$.

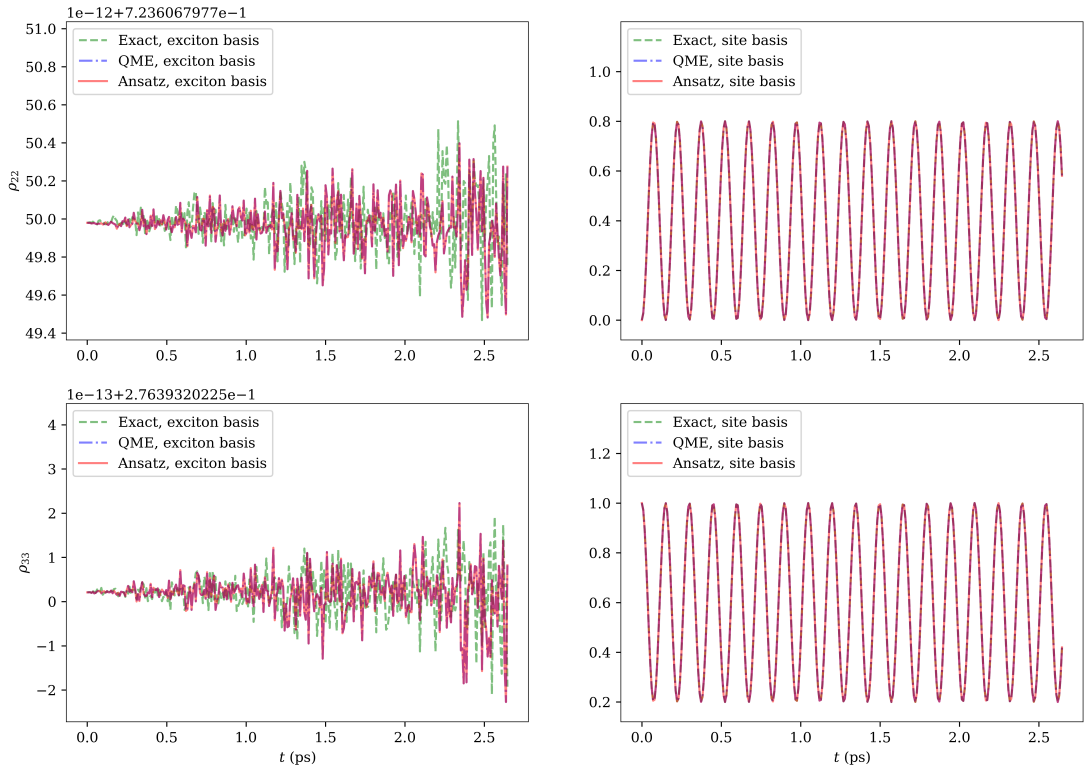

Figure 5.6: The Huang-Rhys factor in the interaction Hamiltonian was set to $S = 0$.

One important observation can be made after looking at the graphs on 5.2 - 5.6, that positivity of the RDM obtained by dynamics involving ansatz is broken, if the simulation is sufficiently long enough. However, plausible results are obtained in the case that the interaction with bath is sufficiently weak.

5.6 The Limit Case of Weak Electronic Coupling

In this section, we will study closely on the dynamics with use of the ansatz for the bath 4.1 with vanishing coupling J in Hamiltonian of the system 3.5. Coupling was set to the values $J \in \{150, 50, 12, 6\}\,\mathrm{cm}^{-1}$. Numerical simulations for the system with ansatz for the bath 4.1 were carried out and compared to the exact dynamics using evolution operators 5.12 and Liouville von Neumann equation 2.16. For a model, we select a dimer model with one LHO coupled to each molecule, and the frequencies are set to $\omega_{1,2} = 100\,\mathrm{cm}^{-1}$. Energies of the molecules are $E_1 = 12500\,\mathrm{cm}^{-1}$ and $E_2 = 12400\,\mathrm{cm}^{-1}$. The Huang-Rhys factor is set to $S_{1,2} = 0.05$. The initial condition was set as a pure state created by laser excitation from the ground electronic and vibrational state in site basis.

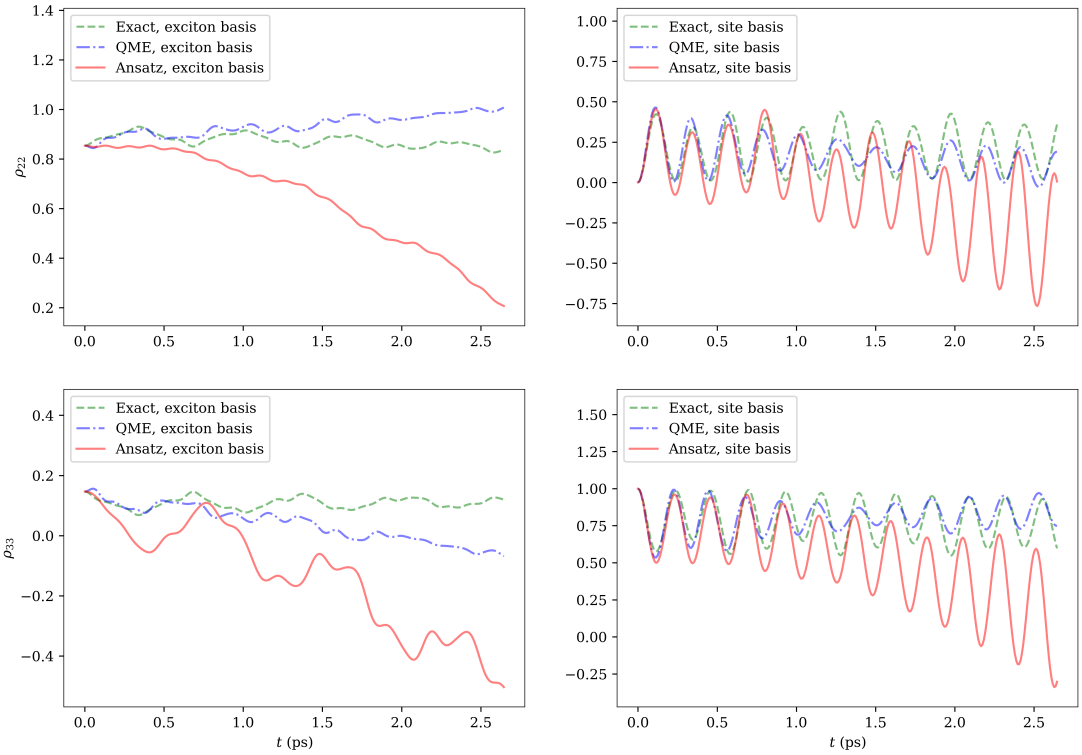

Figure 5.7: Compared dynamics of the exact solution with evolution operators (green, dashed), exact TNL QME (blue, dashdotted) and the ansatz for the bath using TNL QME (red, full). Coupling in the system Hamiltonian was set to $J = 25\,\mathrm{cm}^{-1}$.

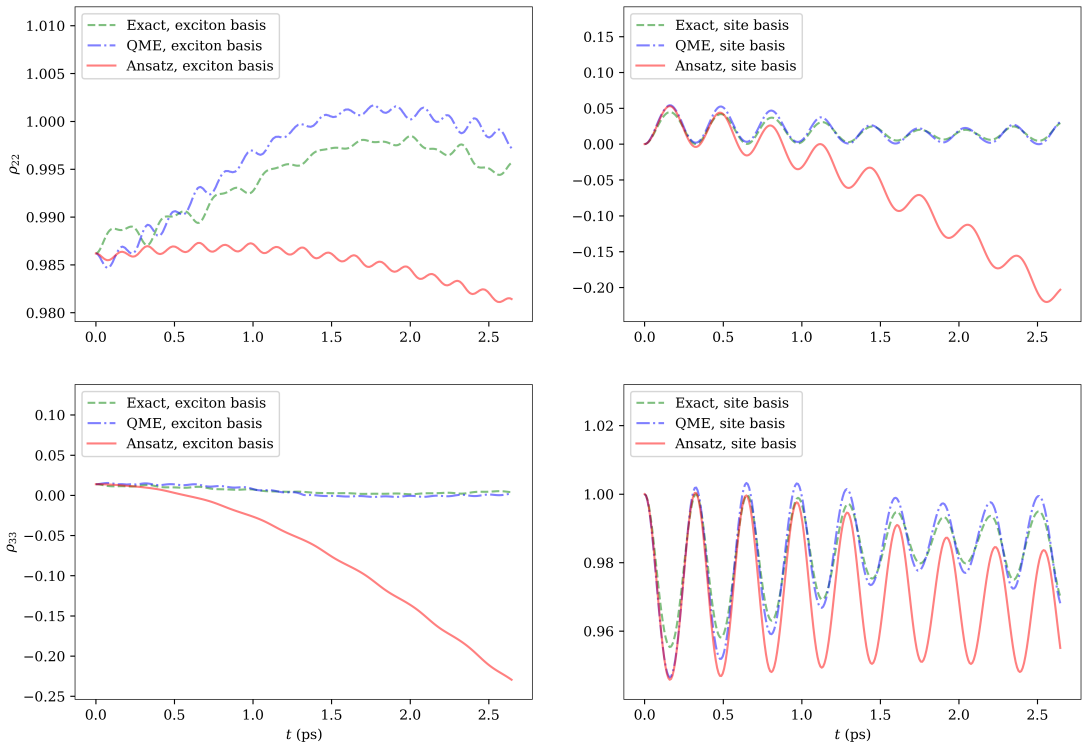

Figure 5.8: Coupling in the system Hamiltonian was set to $J = 12\,\mathrm{cm}^{-1}$.

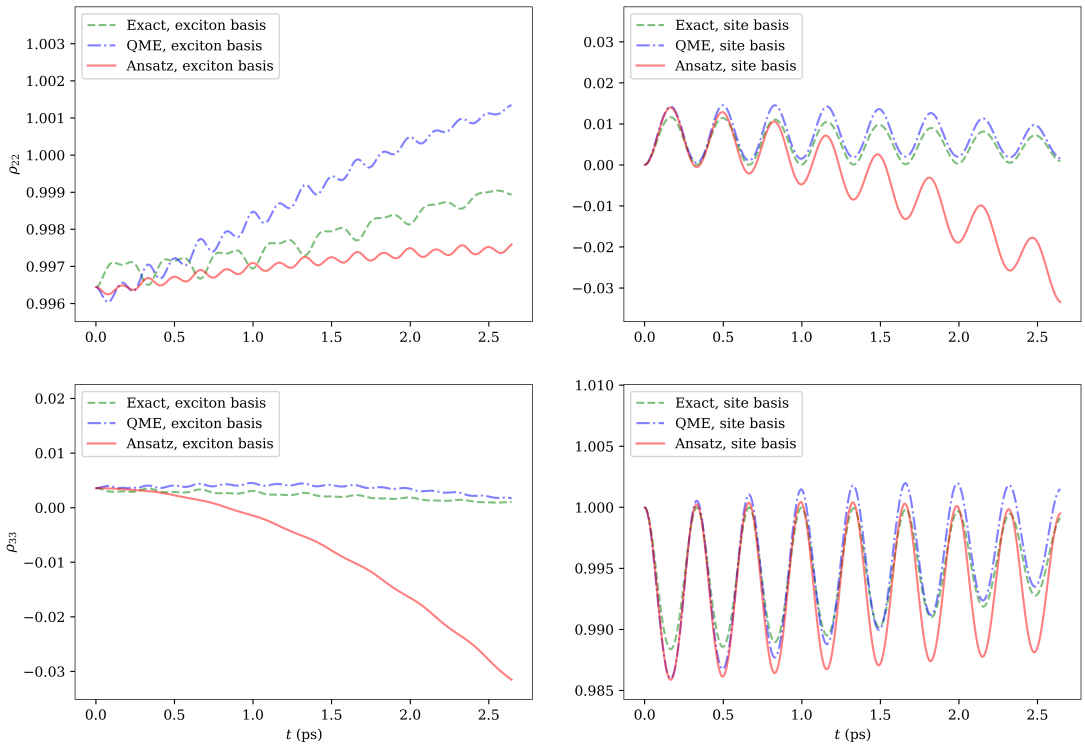

Figure 5.9: Coupling in the system Hamiltonian was set to $J = 6\,\mathrm{cm}^{-1}$.

Looking at 5.7 - 5.9, we can conclude that the dynamics from ansatz resembles

the actual dynamics gradually better with the slower electronic transfer. That can be seen on the time-dependent population ρ_{nn} in excitonic basis.

5.7 Finite Step-Size in Solving Time-Nonlocal Quantum Master Equation

When solving TNL QME it is crucial to find the suitable size of the step. Despite the fact, that it is possible to the use adaptive step-size in solving IDE, due to the relatively small number of steps needed to evaluate such dynamics, we will only use constant step-size. In this section, we will show that $N_{\text{steps}} = 300$ is sufficient and the results are unaffected by the resolution of the solution. The dimer has one LHO coupled to each molecule, and the frequencies are set to $\omega_{1,2} = 100\,\text{cm}^{-1}$. Energies of the molecules are $E_1 = 12500\,\text{cm}^{-1}$ and $E_2 = 12400\,\text{cm}^{-1}$. The Huang-Rhys factor is set to $S_{1,2} = 0.05$ and coupling to $J = 100\,\text{cm}^{-1}$.

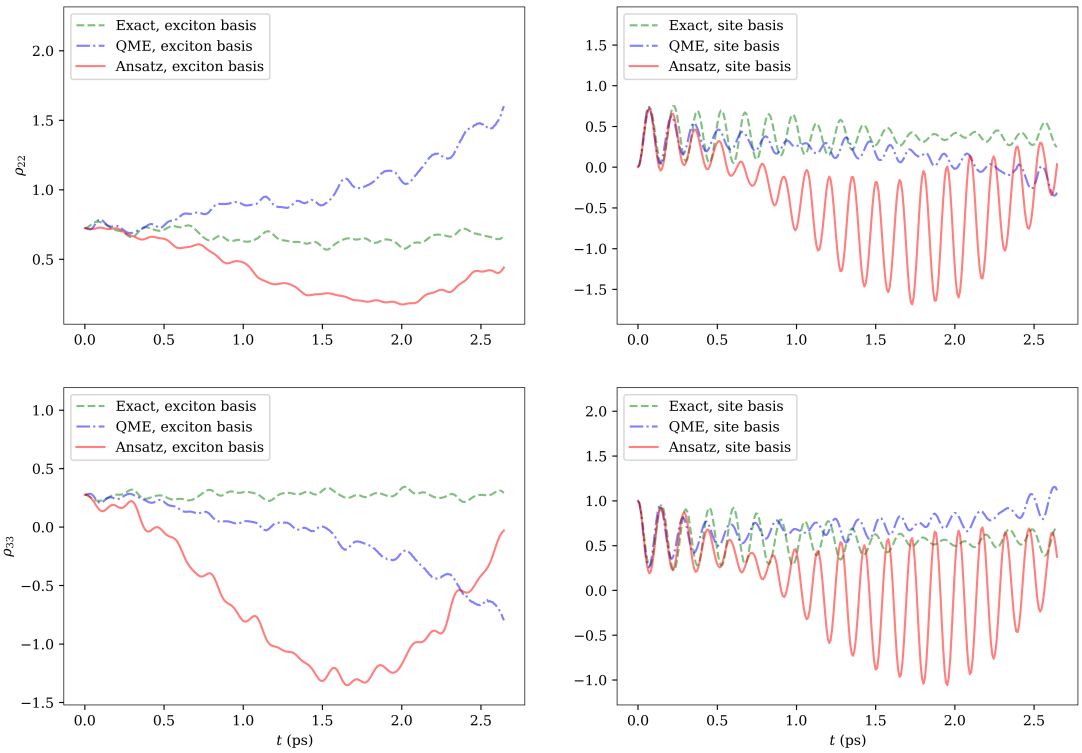

Figure 5.10: Compared dynamics of the exact solution with evolution operators (green, dashed), exact TNL QME (blue, dashdotted) and the ansatz for the bath using TNL QME (red, full). The length of the simulation was set to $t_1 = 2.65$ ps and the number of steps in solving QME is $N_{\text{steps}} = 300$.

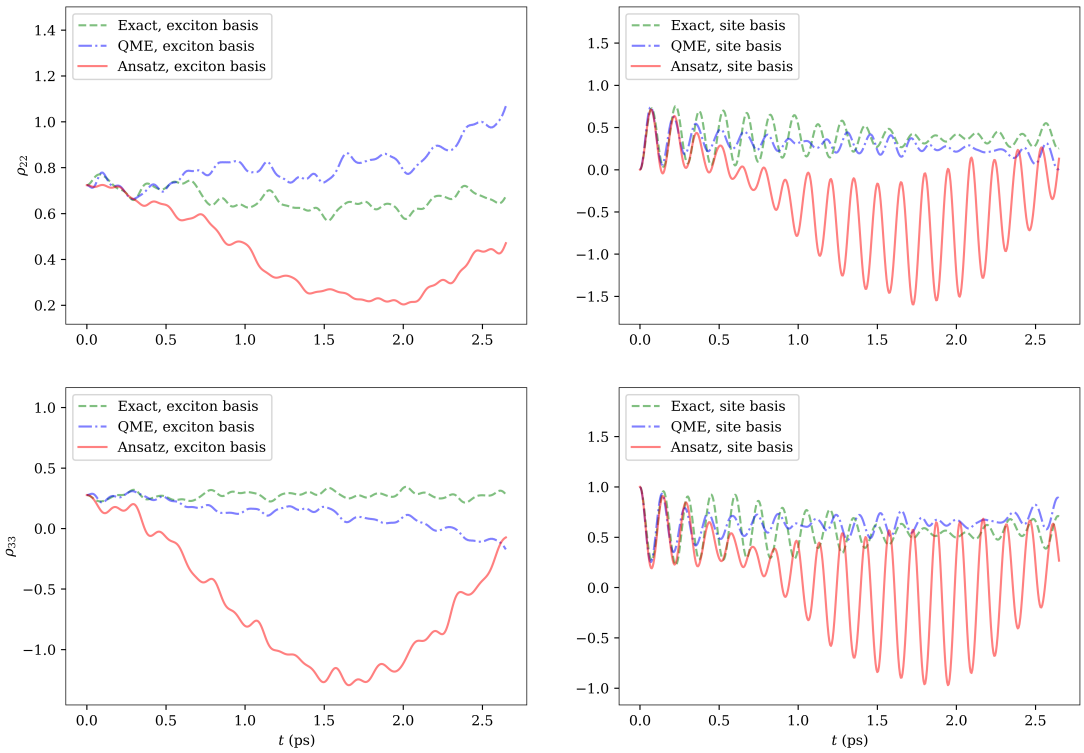

Figure 5.11: The length of the simulation was set to $t_1 = 2.65$ ps and the number of steps in solving QME is $N_{\text{steps}} = 500$.

Changing the number of steps from $N_{\text{steps}} = 300$ to $N_{\text{steps}} = 500$ does not change the character of the QME solution at the graph 5.10 5.11. That justifies the size of step we used for the rest of the TNL QME simulations.

5.8 Slow Dynamics in Exciton Basis

Let us begin with thermalised density matrix W_{eq} at temperature for example $T = 50$ K. Suppose we would be in a position to excite our dimer in exciton basis, and we would assume that the coupling of system and bath is weak. That would certainly lead to very slow and uninteresting dynamics in exciton basis. However, we can test how well will the ansatz of bath in QME be in a position to resemble the original dynamics through the site basis. We will again use the model of the dimer as in previous sections. The frequencies of bath LHOs are set to $\omega_{1,2} = 100\,\text{cm}^{-1}$ and the coupling is set to $J = 100\,\text{cm}^{-1}$. Energies of the molecules are $E_1 = 12500\,\text{cm}^{-1}$ and $E_2 = 12400\,\text{cm}^{-1}$. The Huang-Rhys factor is set to $S_{1,2} = 0.00625$.

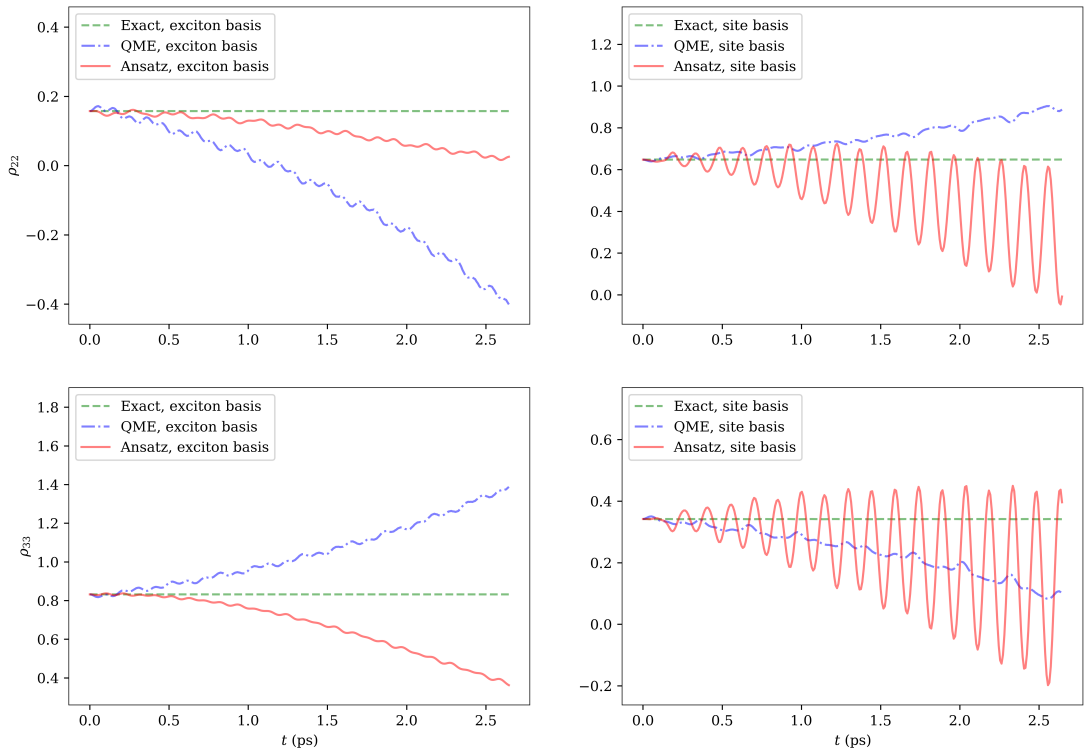

Figure 5.12: Compared dynamics of the exact solution with evolution operators (green, dashed), exact TNL QME (blue, dashdotted) and the ansatz for the bath using TNL QME (red, full). In the beginning, mostly one exciton state is populated due to the strong laser excitation. The coupling with the bath is weak, so the exciton transfer is correspondingly slow.

At figure 5.12 we can see that the TNL QME with ansatz reflect the exact dynamics only for a brief amount of time. In the exciton basis, there seem to be oscillations with a constant amplitude.

5.9 Trimer Model

The certain point of interest to is inspect how well will QME with ansatz reflect the exact dynamics with growing number of the bath DOF. With growing number of DOF, the total basis grows exponentially. However, in QME with relatively narrow basis it is convenient to work with full density matrix rather than with decomposition of density matrix into a set of pure states with weights. On top of that we have to solve convolution in QME so the number of steps to evaluate grows quadratically. To put it into perspective, it takes to run trimer model QME with $N_{\text{steps}} = 300$ for 53.7 hours realtime. The implemented code has been already optimised using vectorization and *OpenBLAST* package on *Intel(R) Core(TM) i7-6700 CPU @ 3.40GHz* single threaded. The excited energies of trimer molecules were set to $E_1 = 12400\ \text{cm}^{-1}$, $E_2 = 12300\ \text{cm}^{-1}$ and $E_3 = 12200\ \text{cm}^{-1}$. The frequency of LHOs in bath were set to $\omega_1 = 90\ \text{cm}^{-1}$, $\omega_2 = 100\ \text{cm}^{-1}$ and $\omega_3 = 110\ \text{cm}^{-1}$. The coupling between molecules was set to $J_{12} = J_{23} = 100\ \text{cm}^{-1}$ and the Huang-Rhys factor was set to $S_{1,2,3} = 0.05$.

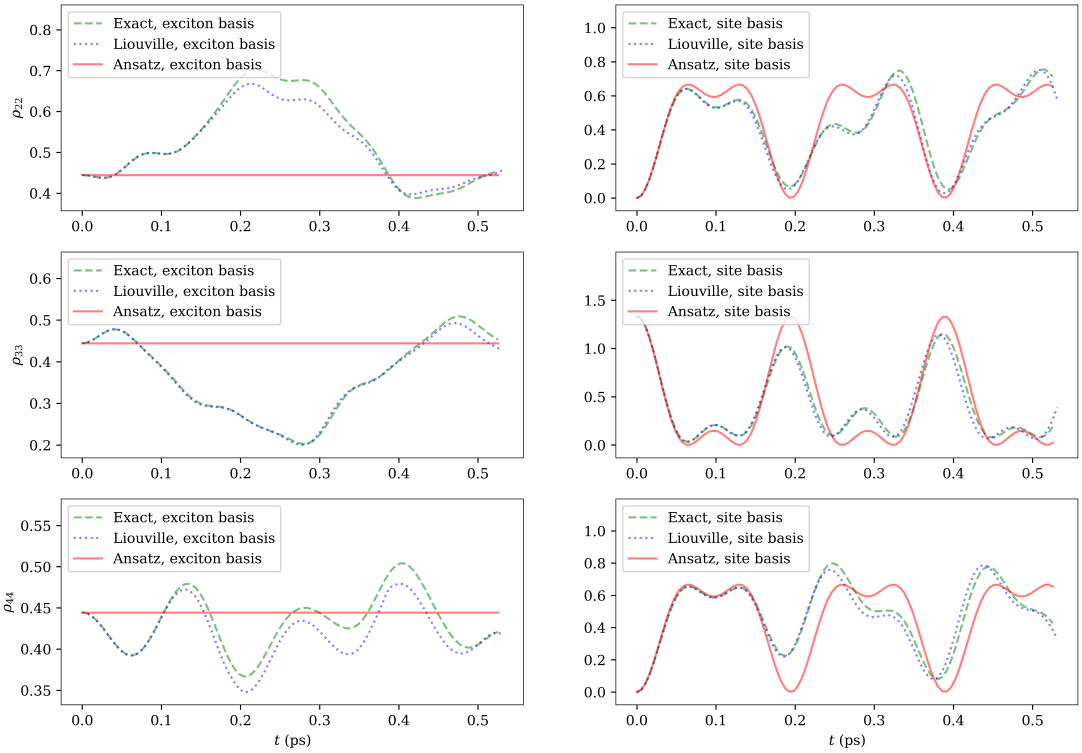

Figure 5.13: Compared dynamics of the exact solution with evolution operators (green, dashed), Liouville von Neumann equation (blue, dotted) and the ansatz for the bath using TNL QME (red, full). The whole system was thermalised and initially excited in excitonic basis.

5.10 Comparison of Exacat Memory Kernel with Approximative Memory Kernel

We strive to analyse the elements of the exact memory kernel and the memory kernel induced by the ansatz for the bath (ansatz memory kernel). For given time variables t and s there are 81 different elements $\mathcal{M}_{abcd}(t,s)$ for the dimer model. Instead of comparing single elements of the exact and ansatz memory kernel, we will inspect whether the same elements are nonzero in both kernels. Memory kernels were calculated before solving of ansatz TNL QME took place.

Starting with a mixed state used in simulation in figure 5.12 the initial RDM matrix does not have any zero elements. We compared both kernels on the whole timescale od simulation, and we have found out that all elements in both kernels are nonzero. In the pure state as an example in the simulation on the figure on 5.5 we have found out that nonzero elements of ansatz $\mathcal{M}_{abcd}(t,s)$ are only that for which elements of RDM $\rho_{ab}(0)$ or $\rho_{cd}(0)$ are nonzero. Also, we observed that the elements $\mathcal{M}_{abcd}(t,s)$ for which $\rho_{ab}(0)$ are nonzero were a few orders lower than the rest of nonzero elements. In the exact memory kernel were all elements nonzero.

6. Conclusion

In this thesis, we focused on the derivation and validation of a more precise description for finite systems than what current approximate methods provide. We hope that this pioneering work will help in consequent improvements of equations of motion for finite systems, which could lead to a better description of systems with infinite baths. The most popular theories for the system with infinite baths have only a limited ability to correctly describe the relaxation, energy transfer and decoherence induced by coupling of the molecular aggregate to the phonon bath on the sub-picosecond time-scales, which are probed by non-linear spectroscopic experiments. This presumably is a very challenging task, and there is still a place for more research in this area.

In the first part of this thesis, we derived a new equation of motion for the open quantum system which describes the electron-phonon interaction. An ansatz for the time evolution of a bath is chosen and incorporated in Quantum Master Equation to derive a set of integrodifferential equations. The ansatz essentially tells us that the bath part of the density matrix with respect to the site basis remains constant. This separation differs from one created using projection superoperators. For any further practical usage of these equations, it is necessary to transform the kernel into a more computationally favourable form. That was done in two distinct ways, and we obtained the so-called Memory kernel of the first kind and Memory kernel of the second kind. The first kernel is suited for small systems where the basis size is sufficiently small due to the slow tracing of bath degrees of freedom. The second kernel is slower to evaluate for the system size of our interest, however, memory kernel can be further used to derive Redfield tensor.

With the derived theory incorporating ansatz for the bath into TNL QME, we implement methods to solve IDE in Julia language. We successfully showed that the ansatz gives for few pico-seconds realistic results even for small systems such as dimer and trimer. The success with mixed states was made only to some extent. The next logical step would be to derive the method for improvement of the memory kernel containing ansatz for the bath without any prior knowledge of the exact solution. This could show us how to iteratively improve the memory kernel only with the knowledge of RDM from the previous step of the iteration.

Bibliography

[Bla95] Robert Blankenship. *Anoxygenic photosynthetic bacteria*. Kluwer Academic Publishers, Dordrecht Boston, 1995.

[BMSF04] Tobias Brixner, Tomáš Mančal, Igor V. Stiopkin, and Graham R. Fleming. Phase-stabilized two-dimensional electronic spectroscopy. *The Journal of Chemical Physics*, 121(9):4221–4236, 2004. Publisher: American Institute of Physics.

[Bre02] Breuer. *The theory of open quantum systems*. Oxford University Press, Oxford New York, 2002.

[BWZ13] Ingemar Bengtsson, Stephan Weis, and Karol Zyczkowski. Geometry of the set of mixed quantum states: An apophatic approach. *arXiv:1112.2347 [quant-ph]*, pages 175–197, 2013. arXiv: 1112.2347.

[CCC+20] Jianshu Cao, Richard J. Cogdell, David F. Coker, Hong-Guang Duan, Jürgen Hauer, Ulrich Kleinekathöfer, Thomas L. C. Jansen, Tomáš Mančal, R. J. Dwayne Miller, Jennifer P. Ogilvie, Valentyn I. Prokhorenko, Thomas Renger, Howe-Siang Tan, Roel Tempelaar, Michael Thorwart, Erling Thyrhaug, Sebastian Westenhoff, and Donatas Zigmantas. Quantum biology revisited. *Science Advances*, 6(14):eaaz4888, April 2020. Publisher: American Association for the Advancement of Science Section: Review.

[Cha08] Jia-Lin Chang. A new method to calculate Franck–Condon factors of multidimensional harmonic oscillators including the Duschinsky effect. *The Journal of chemical physics*, 128:174111, 2008.

[COM04] M. L. Cowan, J. P. Ogilvie, and R. J. D. Miller. Two-dimensional spectroscopy using diffractive optics based phased-locked photon echoes. *Chemical Physics Letters*, 386(1):184–189, 2004.

[Cro18] Roberta Croce. *Light Harvesting in Photosynthesis*. CRC Press, Boca Raton, FL, 2018.

[ECR+07] Gregory S. Engel, Tessa R. Calhoun, Elizabeth L. Read, Tae-Kyu Ahn, Tomáš Mančal, Yuan-Chung Cheng, Robert E. Blankenship, and Graham R. Fleming. Evidence for wavelike energy transfer through quantum coherence in photosynthetic systems. *Nature*, 446(7137):782–786, 2007. Number: 7137 Publisher: Nature Publishing Group.

[Fai02] Benjamin Fain. *Irreversibilities in quantum mechanics*. Kluwer Academic, New York, 2002.

[Fre31] J. Frenkel. On the Transformation of light into Heat in Solids. I. *PhRv*, 37(1):17–44, 1931.

[Gus78] Fred G. Gustavson. Two Fast Algorithms for Sparse Matrices: Multiplication and Permuted Transposition. *ACM Transactions on Mathematical Software (TOMS)*, 4(3):250–269, 1978.

[HJW93] Lane P. Hughston, Richard Jozsa, and William K. Wootters. A complete classification of quantum ensembles having a given density matrix. *Physics Letters A*, 183(1):14–18, 1993.

[Jam72] A. Jamiołkowski. Linear transformations which preserve trace and positive semidefiniteness of operators. *Reports on Mathematical Physics*, 3(4):275–278, 1972.

[Jon03] David M. Jonas. Optical Analogs of 2D NMR. *Science*, 300(5625):1515–1517, 2003. Publisher: American Association for the Advancement of Science Section: Perspective.

[Man20] T. Mančal. A decade with quantum coherence: How our past became classical and the future turned quantum. *Chemical Physics*, 532, 2020.

[May11] Volkhard May. *Charge and energy transfer dynamics in molecular systems*. Wiley-VCH, Weinheim, 2011.

[Nak58] Sadao Nakajima. On Quantum Theory of Transport PhenomenaSteady Diffusion. *Progress of Theoretical Physics*, 20(6):948–959, 1958. Publisher: Oxford Academic.

[Nie10] Michael Nielsen. *Quantum computation and quantum information*. Cambridge University Press, Cambridge New York, 2010.

[Pre92] William Press. *Numerical recipes in C : the art of scientific computing*. Cambridge University Press, Cambridge Cambridgeshire New York, 1992.

[Pri17] Ilya Prigogine. *Non-Equilibrium Statistical Mechanics*. Dover Publications, Mineola, 2017.

[Red65] A. G. Redfield. The Theory of Relaxation Processes. In John S. Waugh, editor, *Advances in Magnetic and Optical Resonance*, volume 1 of *Advances in Magnetic Resonance*, pages 1–32. Academic Press, 1965.

[RN17] Christopher Rackauckas and Qing Nie. Differentialequations. jl–a performant and feature-rich ecosystem for solving differential equations in julia. *Journal of Open Research Software*, 5(1), 2017.

[Sak10] J. J. Sakurai. *Modern Quantum Mechanics (2nd Edition)*. Pearson, 2010.

[Tar05] Albert Tarantola. *Inverse Problem Theory and Methods for Model Parameter Estimation*. Other Titles in Applied Mathematics. Society for Industrial and Applied Mathematics, 2005.

[Val13] Leonas Valkunas. *Molecular Excitation Dynamics and Relaxation*. Wiley, Hoboken, 2013.

[Zwa60] Robert Zwanzig. Ensemble Method in the Theory of Irreversibility. *The Journal of Chemical Physics*, 33(5):1338–1341, 1960. Publisher: American Institute of Physics.

A. Appendices

A.1 Efficient Multiplication of Sparse Matrices

Evaluation of the trace over bath DOF takes into account integrals of the form $\langle a, \nu|\mu, b\rangle$ or with compact indices $\langle a|b\rangle$. These integrals are equal to Franck-Condon factors $w_{ab}^{\nu\mu}$ or using compact indices w_{ab}. Most of the Franck-Condon factors will be inevitably equal to zero as we are working in a locally orthogonal basis. Perhaps there is a better way to store all these factors when it comes to evaluating trace over bath DOF. That being said, we choose a sparse matrix F as a data structure for their storage. We will restrict ourselves to a finite number of states N for the whole system. One property of such matrices is that it is symmetric. We can trivially rewrite 1D FC factor into the integral form

$$\begin{aligned}\langle n|m\rangle =& N_n N_m \int_{-\infty}^{\infty} H_n(\sqrt{\alpha_1}x_1) H_m\left(\sqrt{\alpha_2}x_2\right) \\ & \times \exp\left[-\frac{1}{2}\left(\alpha_1 x_1^2 - \alpha_2 x_2^2\right)\right] \mathrm{d}x,\end{aligned} \tag{A.1}$$

where $H_n(x)$ are Hermite's polynomials, N_n is normalisation factor defined in the following way

$$N_s = \left(\frac{\sqrt{\alpha}}{2^n n! \sqrt{\pi}}\right)^{\frac{1}{2}}. \tag{A.2}$$

Parameter α is a function of the frequency of each LHO

$$\alpha = \frac{\omega}{\hbar}. \tag{A.3}$$

Finally, we can recognise that FC factors of our interest consist of many separated 1D FC factors, the symmetry is apparent. For a trace evaluation concerning two chosen states, one has to evaluate the following

$$\begin{aligned}\rho_{nm}(t) &= \sum_k \rho_{nm} \langle k|n\rangle \langle m|k\rangle \\ &= \sum_k \rho_{nm} F_{kn} F_{mk} \\ &= \sum_k \rho_{nm} P_{nm},\end{aligned} \tag{A.4}$$

where P is a sparse matrix, the so-called FC Product matrix of size $N \times N$ and due to the symmetry of F we can evaluate the matrix P simply as

$$P = F^2. \tag{A.5}$$

The rest of this section is devoted to sparse matrix multiplication. Our chosen type for sparse matrix representation is a Compressed sparse column format (CSC). The reason behind this choice stems in the mean access time, here we assume that the data are roughly equally distributed among rows. In the end, we introduce an algorithm for sparse matrix multiplication of the CSC format [Gus78], see Algorithm 1.

Algorithm 1 Multiplication of CSC type sparse matrices

```
function MATMUL(A::SparseMatrixCSC, B::SparseMatrixCSC)
    (m_A, n_A) ← size(A)
    (m_B, n_B) ← size(B)
    I_A ← A.colptr; J_A ← A.rowval; A ← A.nzval; N_A ← length(A)
    I_B ← B.colptr; J_B ← B.rowval; B ← B.nzval; N_B ← length(B)
    N_C ← N_A + N_B
    I_C ← Array(Int64, n_B+1)
    J_C ← Array(Int64, N_C)
    C ← Array(ComplexF64, N_C)
    i_p ← 1
    x_b ← zeros(Int64, m_A)
    x ← zeros(ComplexF64, m_A)
    for i = 1 to n_B do
        I_C[i] ← i_p
        for j_p = I_A[i] to I_A[i + 1] − 1 do
            j ← J_A[j_p]
            A_val ← A[j_p]
            for k_p = I_A[i] to I_B[i + 1] − 1 do
                k ← J_B[k_p]
                B_val ← B[k_p]
                if (x_b[k] ≠ i) then
                    J_C[i_p] ← k
                    i_p ← i_p + 1
                    x_b[k] ← i
                    x[k] ← A_val B_val
                else
                    x[k] ← x[k] + A_val B_val
                end if
            end for
        end for
        for v_p = I_C[i] to i_p − 1 do
            C[v_p] ← x[J_C[v_p]]
        end for
    end for
end function
```

A.2 Mixed State Decomposition

When it comes to the mixed state represented by matrix density ρ, there are essentially two ways of dealing with consequent dynamics. Suppose we have a fixed orthonormal basis $\{\xi_i\}_{i=1}^N$ in which we represent state $|\psi\rangle$. One can presumably execute a simulation of dynamics with full Liouville equation 2.16 using given initial density matrix. Alternatively, one can decompose an initial density matrix into a convex set of pure states [Bre02] and then execute a simulation with the Schrödinger equation on every pure state separately. Such decomposition of mixed state appears as follows

$$\rho = \sum_{i=1}^{k} p_i \left|\phi_i\right\rangle\!\left\langle\phi_i\right|, \tag{A.6}$$

where $\vec{p} = (p_1, p_2, \ldots, p_k)$ is a probability vector and it is convenient to work with non-normalised states $|\phi_i\rangle$. However, with great power comes great responsibility and the reader should keep in mind that such decomposition does not have to be unique in general [HJW93, Nie10]. In contrast to the classical case, there exist infinitely many decompositions of any mixed state $\rho \neq \rho^2$. The number k can be arbitrarily large, and one can choose his own pure states $|\phi_i\rangle$. However, there exists one distinguished decomposition. By diagonalisation of the density matrix, we find its eigenvalues $\lambda_i \geq 0$ and eigenvectors $|\psi_i\rangle$. Now we can write eigendecomposition of mixed state

$$\rho = \sum_{j=1}^{n} \lambda_j \left|\psi_j\right\rangle\!\left\langle\psi_j\right|. \tag{A.7}$$

The number of such eigenvectors n is the so-called rank of the state *rho*. This is the usual definition of the rank of the matrix, and by accident, it agrees with the definition of rank in convex set theory: the rank of a point in a convex set is the smallest number of pure points needed to form the given point as a mixture [BWZ13].

The difficulty of mixed state diagonalisation depends on two main factors. That is the size N and sparsity of the matrix in which the mixed state is represented. With minor N or sufficient sparsity, the diagonalisation of matrices can be exact. At present, there seem to be many algorithms which solve this task well, e.g. Jacobi Algorithm with $O(N^3)$. However, we aim to decompose mixed states with even greater basis with one advantage, obtained decomposition does not have to be exact. Our criterion for terminating such decomposition is with given error $\epsilon_{\text{err}} > 0$ as follows

$$\left\| \rho - \sum_{i=1}^{r} p_i \left|\psi_i\right\rangle\!\left\langle\psi_i\right| \right\|_F \leq \epsilon_{\text{err}}, \tag{A.8}$$

where $\|\cdot\|_F$ is a Frobenius norm, the number of sufficient pure states can be less than or equal to the number of states in exact decomposition $r \leq n$ and $|\psi_i\rangle$ is orthonormal state in chosen basis. Frobenius norm is defined for $A \in \mathbb{C}^{N\times N}$ as

$$\|A\|_{\text{F}} = \left(\sum_{i=1}^{N} \sum_{j=1}^{N} |a_{ij}|^2 \right)^{\frac{1}{2}}. \tag{A.9}$$

This problem can be split into consecutive steps, where we find one non-normalised state $|\phi_i\rangle$ such that we minimise $|\rho_{k-1} - p_k |\psi_k\rangle\langle\psi_k||_F$ where $\rho_k = \sum_{i=1}^{k} p_i |\psi_i\rangle\langle\psi_i|$. We chose Frobenius norm for the obvious convexity of $|\cdot|_F^2$, because convexity is property which is sufficient for systematic treatment of such optimisation task. Our problem for k-th step of decomposition can be formulated as follows

$$\begin{aligned} \min_{p_k,\, c} \quad & \|\rho_{k-1} - p_k \bar{c} \otimes c\|_F \\ \text{s.t.} \quad & \sum_{i}^{N} |c_i|^2 = 1, \\ & c_k \in \mathbb{C}^N, p_k > 0, \end{aligned} \tag{A.10}$$

where $|psi_k\rangle = \sum_{i=1}^{N} c_{ki} |xi_i\rangle$ and c_k is k-th tensor of rank one $c_k = (c_{k1}, \ldots, c_{kN})$ which represents the amplitudes of state vector elements. Nonlinear optimisation tasks of similar character can be solved with Simplex [Tar05] with Levenberg-Marquardt algorithm or for more robust approach with algorithms of full Newton-type [Pre92]. With even larger size of basis we would advise the reader to use The bootstrap method which belongs into the family of Monte Carlo methods.

A.3 Non-Zero Franck-Condon Factors

Before performing any simulations, it is crucial to obtain a Hamiltonian H of the whole system with respect to a chosen basis $|n\rangle$. Most of this work assumes the basis of size 10^3-10^6. Moreover, these calculations include knowledge of Franck-Condon factors. In this section, we will reveal a more sophisticated way how to obtain all Hamiltonian elements than by doing a naive evaluation of all elements. The element H_{nm} will be nonzero if and only if corresponding Franc-Condon factor $\langle n|m\rangle$ is nonzero. From the nature of the models we are working with, most of the Franck-Condon factors will be zero. Undoubtedly, evaluations of H_{nm} also include different calculations, but we stress the importance of evaluation only nonzero factors.

The system state $|n\rangle$ consists of electron signature and vibrational signature and has a well-defined structure as we discussed previously in 2.3

$$|n\rangle = |a\rangle\,|\xi_n\rangle = |\xi_{g_1}^{\mu_1}\rangle|\xi_{g_2}^{\mu_2}\rangle \ldots |\xi_{g_p}^{\mu_p}\rangle, \tag{A.11}$$

here we assume that there are p molecules in the whole system.

The critical step of this section rests in the factorisation of Franck-Condon factors. We will demonstrate it on an example, in each state the excited molecule differs from one another

$$\begin{aligned} \langle n|m\rangle &= \langle e_k|\langle\xi_n|\xi_m\rangle|e_l\rangle \\ &= \langle\xi_{g_1}^{\mu_1}| \ldots \langle\xi_{e_k}^{\mu_k}| \ldots \langle\xi_{g_p}^{\mu_p}|\xi_{g_1}^{\nu_1}\rangle \ldots |\xi_{e_l}^{\nu_l}\rangle \ldots |\xi_{g_p}^{\nu_p}\rangle \\ &= \langle\xi_{e_k}^{\mu_l}|\xi_{g_k}^{\nu_l}\rangle\langle\xi_{g_l}^{\mu_l}|\xi_{e_l}^{\nu_l}\rangle \prod_{\substack{i=1 \\ i\neq k,l}} \langle\xi_{g_i}^{\mu_i}|\xi_{g_i}^{\nu_i}\rangle \\ &= \langle\mu_k|\hat{D}(\alpha_k)|\nu_k\rangle\ \langle\mu_l|\hat{D}(-\alpha_l)|\nu_l\rangle \prod_{\substack{i=1 \\ i\neq k,l}} \langle\mu_i|\hat{D}(0)|\nu_i\rangle\,. \end{aligned} \tag{A.12}$$

Here we used the notation for Franck-Condon factors from the section 2.5. For the ease of notation, we will use the following compact form of 1D Franck-Condon factors

$$F_{ij}^{\alpha} \equiv \langle i|\hat{D}(\alpha)|j\rangle\,. \tag{A.13}$$

More importantly, most of the factors $F_{\mu_i\nu_i}^{\alpha_i}$ in the last product of equation A.12 will be zero, more precisely $F_{mu_inu_i}^{0} \neq 0$ if and only if $i = j$. Perhaps the better way of evaluating these factors a priori is to save nonzero $F_{mu_inu_i}^{\alpha_i}$ and then as a result iterate only over the nonzero factors in creating multidimensional Franck-Condon factor $\langle n|m\rangle$, see Algorithm 2.

A.4 Efficient Calculation of Multidimensional Franck-Condon Factors

Evaluating 1D Franck-Condon factors can be done in many different ways. One dimensional LHO wave-functions can be described as

$$|n\rangle = N_n H_n(\sqrt{\alpha}x)\exp\left(-\frac{1}{2}\alpha x^2\right), \quad N_n = \left(\frac{\sqrt{\alpha}}{2^n n!\sqrt{\pi}}\right)^{\frac{1}{2}}, \tag{A.14}$$

where N_n is normalization factor, $H_n(x)$ is Hermite's polynomial and α is reduced frequency

$$\alpha = \frac{\omega}{\hbar}. \tag{A.15}$$

As the reader is probably expecting, the Franck-Condon factor can be rewritten to the following integral

$$\langle n|m\rangle = N_n N_m \int_{-\infty}^{\infty} H_n(\sqrt{\alpha_1}x_1)H_m\left(\sqrt{\alpha_2}x_2\right)\exp\left[-\frac{1}{2}\left(\alpha_1 x_1^2 + \alpha_2 x_2^2\right)\right]\mathrm{d}x, \tag{A.16}$$

where $x_1 = x$ and $x_2 = x + d$. Without any doubt, this integral is not the end point, in work [Cha08] Chang successfully has rewritten this integral into partial sums of Hermite's polynomials as follows. Now we choose substitutions

$$\begin{array}{ll} K = \exp\left(-\frac{\alpha_1\alpha_2 d^2}{2(\alpha_1+\alpha_2)}\right) & y = x + \frac{\alpha_2 d}{\alpha_1+\alpha_2} \\ \beta_1 = -\frac{\sqrt{\alpha_1}\alpha_2 d}{\alpha_1+\alpha_2} & \beta_2 = -\frac{\alpha_1\sqrt{\alpha_2},d}{\alpha_1+\alpha_2} \end{array} \tag{A.17}$$

and due to the property of Hermite's polynomials

$$H_n(x+y) = \sum_{k=0}^{n}\binom{n}{k}H_k(x)(2y)^{(n-k)} \tag{A.18}$$

we can rewrite A.16 using substitutions into the following form

$$\begin{aligned} \langle n|m\rangle = N_n N_m K \int_{-\infty}^{\infty} & H_n(\sqrt{\alpha_1}y + \beta_1)H_m\left(\sqrt{\alpha_2}y + \beta_2\right) \\ & \times \exp\left(-\frac{1}{2}(\alpha_1+\alpha_2)y^2\right)\mathrm{d}y, \end{aligned} \tag{A.19}$$

Algorithm 2 Evaluation of multidimensional Franck-Condon factors

```
calculate Franck-Condon factors F^{α_i}_{μ_i ν_i} and F^{-α_i}_{μ_i ν_i}
and save all (μ, ν) for F^α_{μν} ≠ 0 into M_α
function CORE(i, nState, mState, fc)
    (e_ni, e_mi) ← (0, 0)
    if nState.excited == i then e_ni = 1 end if
    if mState.excited == i then e_mi = 1 end if
    α = α_i(e_ni − e_mi)
    for (μ_i, ν_i) in M_α do
        (nCopy, mCopy) ← (nState, mState)
        insert e_ni into nCopy.elState and e_mi into mCopy.elState
        insert μ_i into nCopy.vibState and ν_i into mCopy.vibState
        fcNew ← fc*F^α_{μ_i ν_i}
        if i == p then
            yield (nCopy, mCopy, fcNew)
        else
            yield FORK(i+1, nCopy, mCopy, fcNew)
        end if
    end for
end function
function FORK(i, nState, mState)
    yield CORE(i, nState, mState, fc)
    if nState.excited == 0 then
        nCopy ← nState
        nCopy.excited = i
        yield CORE(i, nCopy, mState, fc)
    end if
    if mState.excited == 0 then
        mCopy ← mState
        mCopy.excited = i
        yield CORE(i, nState, mCopy, fc)
    end if
    if nState.excited == 0 and mState.excited == 0 then
        (nCopy, mCopy) ← (nState, mState)
        nCopy.excited = i; mCopy.excited = i
        yield CORE(i, nCopy, mCopy, fc)
    end if
end function
initialise empty nState and mState
save all FC factors with FORK(1, nState, mState, 1)
```

using the property in A.18 we obtain

$$\begin{aligned}\langle n|m\rangle = N_v N_m K \sum_{k=0}^{n}\sum_{l=0}^{m}\binom{n}{k}\binom{m}{l} H_{n-k}(\beta_1)H_{m-l}\left(\beta_2\right) \\ \times \left(2\sqrt{\alpha_1}\right)^k \left(2\sqrt{\alpha_2}\right)^l \int_{-\infty}^{\infty} y^{k+l}\exp\left(-\frac{1}{2}(\alpha_1+\alpha_2)y^2\right)\mathrm{d}y.\end{aligned} \tag{A.20}$$

The last integral in this equation A.20 is Gaussian integral and it is nonzero when $k+l$ is even

$$\int_{-\infty}^{\infty} x^{2n}e^{-ax^2}dx = \frac{(2n-1)!!}{(2a)^n}\sqrt{\frac{\pi}{a}} \tag{A.21}$$

after some rearrangement, we will be left with the final formula

$$\begin{aligned}\langle n|m\rangle = K\left(\frac{\sqrt{\alpha_1+\alpha_2}}{\alpha_1+\alpha_2}\frac{2}{2^{n+m}n!m!}\right)^{1/2}\sum_{k=0}^{n}\sum_{l=0}^{m}\binom{n}{k}\binom{m}{l}H_{v-k}(\beta_1)H_{m-l}\left(\beta_2\right) \\ \times \left(2\sqrt{\alpha_1}\right)^k\left(2\sqrt{\alpha_2}\right)^l C(k+l),\end{aligned} \tag{A.22}$$

where multiplication constant $C(k+l)$ is defined as

$$C(n) = \begin{cases}\frac{(n-1)!!}{(\alpha_1+\alpha_2)^{n/2}} & n = 1, \text{n is even} \\ 0 & \text{otherwise.}\end{cases} \tag{A.23}$$

We recognise this as an opportunity in case higher orders of Franck-Condons factors have to be evaluated; however, in our case we are working with a limited amount of LHO eigenstates, that is $N \leq 12$. It is convenient to use the formula

$$\langle i|\hat{D}(d)|j\rangle = \langle i|\exp\left[-\frac{d}{\sqrt{2}}\left(\hat{a}-\hat{a}^\dagger\right)\right]|j\rangle\,, \tag{A.24}$$

here the shift is denoted with the variable d. Inside A.24 we are calculating exponential of matrix, sufficiently large size of the basis N has to be chosen for the convergence of $\langle i|\hat{D}_d|j\rangle$ in a smaller basis of size n. For numerical approval of this method we select Frobenius norm, so that the change in k-th step of convergence is defined as

$$\delta_k = \left(\sum_{i=1}^{n}\sum_{j=1}^{n}\left|F_{ij}^k - F_{ij}^{k-1}\right|^2\right)^{1/2}, \tag{A.25}$$

where F_{ij}^k is Franck-Condon factor evaluated with k elements of basis.

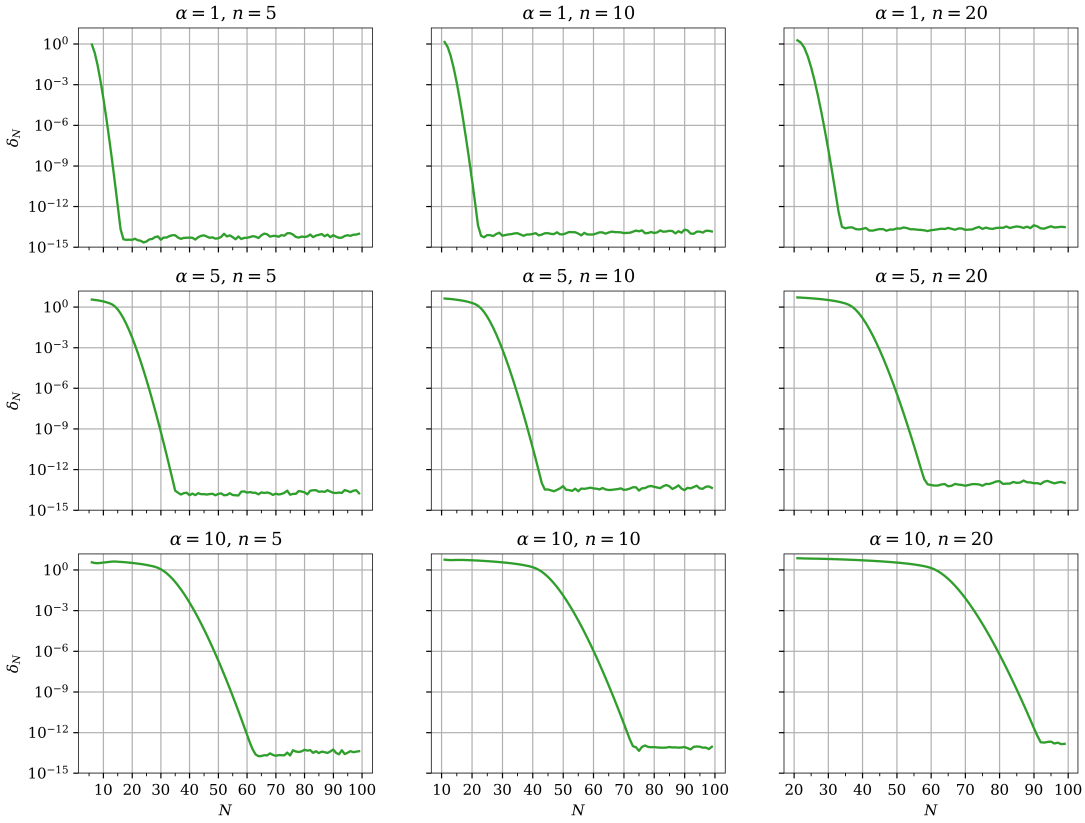

Figure A.1: Convergence of Franck-Condon factors calculated using an exponential of shift operators. On each figure we can observe the absolute change of relevant Franck-Condon factors with Frobenius norm.